Star Shaped Silver Nanoparticles For Titanium Implant Coatings

By

Aqsa Mushtaq

(Registration No: 00000401717)

Department of Biomedical Sciences

School of Mechanical and Manufacturing Engineering

National University of Sciences & Technology (NUST)

Islamabad, Pakistan

(2024)

Star Shaped Silver Nanoparticles For Titanium Implant Coatings

By

Aqsa Mushtaq

(Registration No: 00000401717)

A thesis submitted to the National University of Sciences and Technology, Islamabad,

In partial fulfillment of the requirements for the degree of

Master of Science in
Biomedical Sciences

Supervisor: Dr. Nosheen Fatima

School of Mechanical and Manufacturing Engineering

National University of Sciences & Technology (NUST)

Islamabad, Pakistan

(2024)

THESIS ACCEPTANCE CERTIFICATE

Certified that final copy of MS/MPhil thesis written by **Regn No. 00000401717 Aqsa Mushtaq** of **School of Mechanical & Manufacturing Engineering (SMME)** has been vetted by undersigned, found complete in all respects as per NUST Statues/Regulations, is free of plagiarism, errors, and mistakes and is accepted as partial fulfillment for award of MS/MPhil degree. It is further certified that necessary amendments as pointed out by GEC members of the scholar have also been incorporated in the said thesis titled. **Star Shaped Silver Nanoparticles For Titanium Implant Coatings**

Signature:

Name (Supervisor): Nosheen Fatima Rana

Date: 03 - Sep - 2024

Signature (HOD):

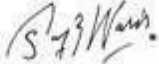Date: 03 - Sep - 2024

Signature (DEAN):

Date: 03 - Sep - 2024

National University of Sciences & Technology (NUST)
MASTER'S THESIS WORK

We hereby recommend that the dissertation prepared under our supervision by: Aqsa Mushtaq (00000401717)
Titled: Star Shaped Silver Nanoparticles For Titanium Implant Coatings be accepted in partial fulfillment of the requirements for the award of MS in Biomedical Sciences degree.

Examination Committee Members

1. Name: Muhammad Asim Waris   Signature:

2. Name: Aneeqa Noor   Signature:

3. Name: Mehak Rafiq   Signature:

Supervisor: Nosheen Fatima Rana   Signature:

Date: 03 - Sep - 2024

03 - Sep - 2024

Head of Department   Date

COUNTERSINGED

03 - Sep - 2024

Date   Dean/Principal

CERTIFICATE OF APPROVAL

This is to certify that the research work presented in this thesis, entitled "Star Shaped Silver Nanoparticles For Titanium Implant Coatings" was conducted by Ms. Aqsa Mushtaq under the supervision of Dr. Nosheen Fatima. No part of this thesis has been submitted anywhere else for any other degree. This thesis is submitted to the School of Mechanical and Manufacturing Engineering in partial fulfillment of the requirements for the degree of Master of Science in Field of Biomedical Sciences Department of Biomedical engineering and Sciences, National University of Sciences and Technology, Islamabad.

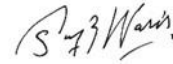Student Name: Aqsa Mushtaq   Signature: _____

Supervisor Name: Dr. Nosheen Fatima Rana   Signature: _____

Name of Dean/HOD: Dr. Muhammad Asim Waris   Signature: _____

AUTHOR'S DECLARATION

I <u>Aqsa Mushtaq</u> hereby state that my MS thesis titled "Star Shaped Silver Nanoparticles For Titanium Implant Coatings" is my own work and has not been submitted previously by me for taking any degree from National University of Sciences and Technology, Islamabad or anywhere else in the country/ world. At any time if my statement is found to be incorrect even after I graduate, the university has the right to withdraw my MS degree.

Name of Student: <u>Aqsa Mushtaq</u>

Date: <u>03-09-2024</u>

PLAGIARISM UNDERTAKING

I solemnly declare that research work presented in the thesis titled "Star Shaped Silver Nanoparticles For Titanium Implant Coatings" is solely my research work with no significant contribution from any other person. Small contribution/ help wherever taken has been duly acknowledged and that complete thesis has been written by me.

I understand the zero tolerance policy of the HEC and National University of Sciences and Technology (NUST), Islamabad towards plagiarism. Therefore, I as an author of the above titled thesis declare that no portion of my thesis has been plagiarized and any material used as reference is properly referred/cited.

I undertake that if I am found guilty of any formal plagiarism in the above titled thesis even after award of MS degree, the University reserves the rights to withdraw/revoke my MS degree and that HEC and NUST, Islamabad has the right to publish my name on the HEC/University website on which names of students are placed who submitted plagiarized thesis.

Student Signature:

Name: Aqsa Mushtaq

I dedicate this work to my parents whose never ending love, firm support and endless prayers have been the foundation of all my achievements, their Encouragement has guided me through every challenge, their strong belief in me has been a constant source of strength for me. I owe every success to their sacrifices and wisdom. "Their unwavering support has made this journey possible, and for that I am forever grateful.

ACKNOWLEDGEMENTS

TABLE OF CONTENTS

LIST OF FIGURES

LIST OF ABBREVIATIONS, SYMBOLS AND ACRONYMS

SBF	Simulated Body fluids
TSA	Tryptic soy agar
TSB	Tryptic soy broth
SEM	Scanning electron microscopy
FTIR	Fourier transform infrared spectroscopy
XRD	X-ray Diffraction
NaOH	Sodium Hydroxide
UTS	Ultimate tensile strength
AgNPs	Silver nanoparticles
AgNSs	Silver Nanostars
AgNo3	Silver Nitrate
PVP	Polyvinylpyrolidone
PEG	Poly Ethylene Glycol
PCA	Photo catalytic activity
PDA	Polydopamine
ROS	Reactive Oxygen species
UV	Ultraviolet
HA	Hydroxyapatite

ABSTRACT

Titanium implants are extensively used in the medical and healthcare industries because of their exceptional mechanical strength and biocompatibility. However, there are still concerns with reducing infection and enhancing implant integration with the surrounding bone tissue. In order to improve the antibacterial and biocompatibility of titanium implants, this study prepares star like silver nanoparticles and coat them on titanium discs (Ti-6Al-4V). The process of creating silver nanostars involved heating polyvinylpyrrolidone (PVP) and ethylene glycol solution along with silver precursor solution at 190°C for 30 minutes and reducing silver nitrate with 4×10^{-2} M NaOH. PVP and ethylene glycol were used to stabilize the nanostar. Different properties of nanoparticles such as Surface morphology, functional groups, chemical composition, phase and purity, visual characterization, surface charge and stability were characterized by using SEM, FTIR, Raman spectroscopy, XRD, UV-Vis spectroscopy and zeta analysis. To enhance surface qualities, titanium discs were heated and given alkaline treatments. Simulated body fluid (SBF) and nanostar-coated discs interacted, and contact angle was measured in order to test biocompatibility. The antibacterial efficacy of tryptic soy broth (TSB) and TSA was evaluated against Staphylococcus aureus and there was a significant decrease in biofilm activity observed on 96 well plate.7 days and 14 days coated disc shows 83% and 95% inhibition to biofilm and there was a decrease in contact angle of both discs with increasing coating period, and 14 day coated disc shows contact angle of 22° indicating high hydrophilicity that leads to better Osseo integration and biocompatibility. These findings demonstrated that the silver nanostar coatings considerably increased the antibiofilm activity and make titanium implants more bio absorbable, which may promote Osseo integration and decrease bacterial adherence. This work demonstrates the effectiveness of coatings of silver nanoparticles, marking a significant advance in clinical applications.

Keywords: Silver nanostars, coated titanium disc, biofilm inhibition, biocompatibility, infection control

CHAPTER 1: INTRODUCTION

1.1 Titanium Implants

Bone and joint pathology is implicated in about half of chronic illnesses in European patients over 65. Because of the steady aging of society, it is especially serious. In the European Union, taking into account its 28 member states, it is projected that by 2030, roughly 27% of citizens will be over 65, and that number will increase fivefold within 40 years [1]. The need for a variety of implants is increasing as a result of this circumstance. The information that is currently available regarding the patients dealing with these issues reveals that, according to WHO data, 75 million people worldwide suffer injuries each year; of those victims, 10–30% are still unable to walk, and five million are fatal [2]. One of the main causes of disability is injuries to the locomotion system, primarily to the limbs. Four million people are thought to still be permanently or temporarily disabled as a result of these kinds of disabilities. Due to developments in material science and medicine over the past few decades, a multitude of biomaterials with attributes appropriate for a range of uses have been created [3]. The primary applications of biomaterials are in the fields of orthopedics, dentistry, medication delivery, skin tissue engineering, and cardiovascular devices. Prior to identifying any substance as an implant, it is essential to ascertain that it is biocompatible with the human body and not causing any harm. Certain properties are required of metals that are frequently used in biomedical applications: they must be highly resistant to corrosion and be nontoxic, non-immunogenic, thrombogenic, and carcinogenic. Body fluids are rich in different amino acids, proteins, and chloride ions, which cause corrosion phenomena. Various oxide-reduction reactions occur between metallic surfaces and biological fluid, resulting in their modification and potential release of ions within the body. Numerous adverse effects, including allergies and carcinoma, may result from this.

William Gregor, a British chemist, mineralogist, and clergyman, made the initial discovery of titanium in 1791. Martin Klaproth, a Berlin scientist, independently discovered titanium oxide four years later. The story of the Greek mythological Titans, the progeny of Uranos and Gaia, gave him the inspiration to name it Titanium. Like the hard-to-extract mineral, the Titans were trapped in the earth's crust, completely loathed by their father. It took more than a century to separate the metal. The most common alloy in use today is Ti-6Al-4V, which was developed in the US in the late 1940s. Since several titanium alloys have been developed, light metals are now widely used in a variety of industrial applications [4]. Due to its superior mechanical and chemical properties,

titanium (Ti) and its alloys have been the main materials utilized for implants in orthopedics and dentistry. Titanium has become more and more popular because of its remarkable combination of strength, Young's modulus, and biocompatibility when compared to other metallic implant materials.

1.2 Physical properties of Titanium

- Since titanium is a transition metal, it can combine with other elements' atoms of comparable size to form solid solutions. Up to 882.5 °C, its solid state exhibits its hexagonal close-packed geometry, or α structure. Above this temperature, solid titanium becomes the body-centered cubic β structure, which melts at 1688 °C [5].

- Its lightweight design and low density of 4.5g/cm³ make it an extremely sought-after material for applications where weight reduction is critical, such as in aircraft and medical implants. The low density of titanium implants significantly reduces the overall load and movement inertia on the human body [6].

- Titanium has favorable thermal properties, including a high melting point of about 3034 °F (1668 °C). The material can withstand high temperatures during manufacture without losing its structural integrity because of its high melting point. Moreover, titanium expands and contracts very little due to temperature changes because of its low coefficient of thermal expansion. This feature is advantageous for applications such as precision medical devices where dimensional stability is crucial.

- Because titanium is a relatively weak electrical conductor in comparison to materials like copper or aluminium, it can be useful in applications where electrical insulation is required. In certain medical applications, titanium's low electrical conductivity can be helpful in preventing undesirable electrical interactions with the body's tissues [7].

- Titanium and its alloys are far less rigid than other metallic implants like stainless steel or Co-Cr-Mo alloys. This is beneficial because it can enhance load distribution, promote natural bone formation, and decrease the stress shielding effect [8].

1.3 Chemical properties of Titanium

- Titanium naturally forms a protective oxide layer in oxidizing environments due to its affinity for oxygen. This oxide layer is necessary for titanium to be biocompatible and

corrosion-resistant, particularly at high temperatures. The thickness of titanium's natural oxide layer varies depending on exposure circumstances and alloy composition; it usually ranges from a few nanometres to roughly 10–30 nm. The bulk of composite layers of titanium (IV), titanium (III), and titanium (II) oxides are formed by alloys that are exposed to humid air at ambient temperature [9].

- Titanium is considered biocompatible because of its low electrical conductivity, which facilitates the electrochemical oxidation process and the formation of a thin passive oxide layer. Strong corrosion resistance is the outcome of the oxide layer [10].

1.4 Biological Properties of Titanium

- Dr. Brånemark noted that bone can grow and adhere to titanium alloy surfaces, to the extent that over time, titanium-based devices can undergo complete Osseo integration [11, 12]. One

  Important biomedical property of titanium is its ability to integrate with bone. A variety of biomedical devices, including scaffolds, use this property to improve adhesion and stabilization or to speed up the regeneration of bone tissue. The fact that titanium is thought to be hypoallergenic, meaning that patients rarely experience allergic reactions is another characteristic linked to the presence of native oxides.

- Although titanium is generally non-toxic, wear and corrosion can occasionally result from titanium dental implants, which can deposit particles and ions of titanium and titanium alloy components in the surrounding tissues, causing inflammatory reactions [13]. Utilizing optimized titanium alloys and biocompatible surface coatings (like hydroxyapatite) can lessen ion release and increase compatibility in order to address titanium toxicity. Anodization and nano-structuring are two surface modifications that improve cellular responses.

1.5 Structural properties of Titanium

The mineral sources of titanium oxides are rutile, brookite, and anatase. The crystal structures of rutile, anatase, and brookite are tetragonal, orthorhombic, and belong to space groups P42/mnm, I41/amd, and Pbca, respectively [14]. With the highest refractive index, the rutile structure is thermodynamically more stable than the others. At 882.5 °C, titanium experiences an allotropic

phase transition that results in a shift in its crystal structure from a densely packed hexagonal (alpha phase) to a body-centered cubic (beta phase).
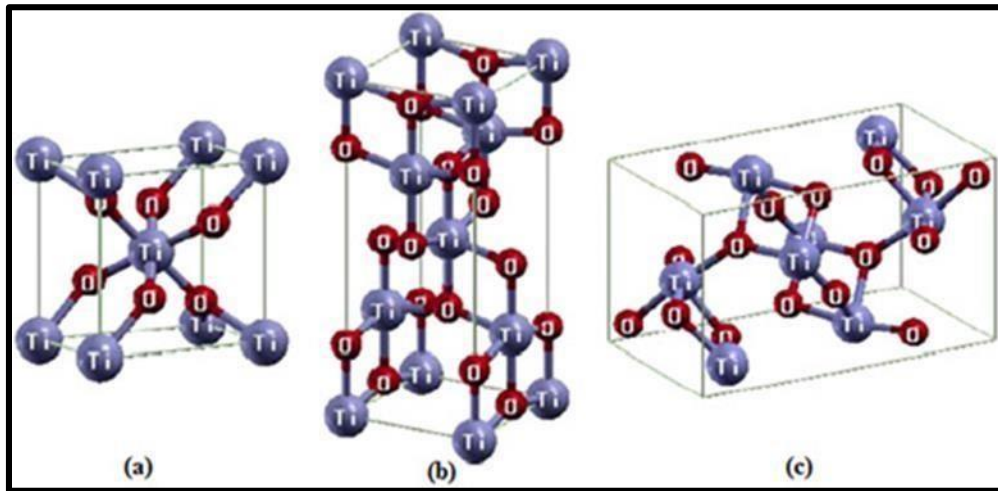
Figure 1.1. Crystal structure of TIO2 (a) Rutile (B) Anatase (c) Brookite Rutile and anatase are the tetragonal crystal systems with different arrangements while brookite has orthorhombic crystal structure

1.6 Classification of Titanium alloys

Based on their crystal structure and the elements added to them, titanium alloys are classified into three groups: α alloys, α+β alloys, and β alloys

1.6.1 α Alloys

These are formed from elements such as tin (Sn) and aluminum (Al), which at low temperatures stabilize the α phase and give the alloy a hexagonal close-packed (hcp) crystal structure.

1.6.2 Near α Alloys

Near-α alloys are α alloys with trace amounts (roughly 1 to 2 weight percent) of β stabilizers that stabilize 5–10% of the β phase into the structure at room temperature. The β phase allows for control over the scale, morphology, and distributions of the two phases, which in turn allows for two-phase strengthening. Among all Ti-alloys, near-α alloys exhibit the strongest resistance against creep at temperatures exceeding 400°C, which is why they are extensively utilized in the compressor section due to its high operating temperature [15].

1.6.3 α+β Alloys

These alloys are composed of stabilizing elements α and β. Elements such as vanadium (V), molybdenum (Mo), niobium (Nb), or chromium (Cr) stabilize the β phase, whereas aluminum stabilizes the α phase. By adding these β stabilizers, the temperature at which the β phase starts to change is lowered and the range where both phases coexist is expanded.

1.6.4 β Alloys

The alloy can maintain the stability of the β phase at room temperature (RT) if sufficient β stabilizers are added. These alloys are known as metastable β because the β phase remains stable even after being cooled in air. Adding additional β stabilizers turns the alloy into a stable β alloy that, even after heat treatments, cannot be converted back to the α+β mixture[16].

1.6.5 Grade 5 Titanium All

The mechanical properties of titanium that is commercially pure and of biomedical grade are generally regarded as being below the ideal range for total joint replacement. As a result, annealed Ti-6Al-4V was first introduced early on and is still the largest titanium alloy used in the production of biomedical devices today [11a]. Ti-6Al-4V is a titanium alloy with a (alpha + beta) composition consisting of 6% aluminium and 4% vanadium. It is widely used in the aerospace, petrochemical, biomedical, and other industries due to its low density, high specific strength, remarkable corrosion resistance, and good welding performance. Actually, more than half of the titanium consumed globally now comes from its use [17].

Figure1.2.Medical applications of Grade 5 Titanium alloy, Figure shows the different types of implants used as orthopedic, dental, hip joint, knee joint replacements and for cardiac stunts.

,

1.7 Temperature's effect on Ti-6Al-4V alloy properties

The thermal conductivity triples between 10°C and 1200°C, while hardness increases with decreasing temperature [17]. When the temperature is changed from room temperature to liquid nitrogen, the tensile strength increases from 1000 to 1700 MPa. Young's modulus decreases as temperature increases above 200°C. At 25°C, the ultimate tensile strength (UTS) was 1000 MPa; at 450°C, it was around 625 MPa, a 45% worldwide drop. The shape, volume fraction, and distribution of Ti–6Al–4V, a common α + β titanium alloy, play a major role in determining its mechanical properties. It possesses some β phase and a sizable quantity of α phase [18].

1.8 Applications of Ti-6Al-4V alloy in medical devices

Titanium alloys are utilized to replace damaged hard tissue in implant devices. Examples include prosthetic cardiac valves, pacemakers, bone plates, screws for mending fractures, artificial knee

and hip joints, and artificial hearts. Titanium and its alloys are also used to make crowns, bridges, over dentures, implants, and components of dental implant prostheses (abutment and screw). There are three types of dental implants: Osseo integrated, mini-implants for orthodontic anchoring, and zygomatic. Each group needs to be made of titanium alloys, or cp Ti, and has distinct mechanical criteria [19].

1.9 Surface chemistry of Ti and Ti alloys

Commercially pure titanium, or cpTi, and Ti-6A1-4V are the two main alloys utilized to construct implantable devices. TiO_2 oxide makes up most of their surfaces. This 4-6 nm thick oxide layer contains hydroxyl groups with oxide [20]. Titanium implants usually undergo surface modification after fabrication to guarantee even oxidation and eliminate unwanted impurities. The enhanced biological characteristics of the resulting surfaces promote bone bonding by promoting cell adhesion and proliferation [21]. Surface roughness and polish of titanium implants are also important factors because of how they affect the quality of their contact with the bone. Surface roughness can be measured using the terms SA, or the arithmetic mean of the roughness area from the mean plane, and Sds, or the density of peaks per unit of area. Based on surface roughness and Sa values, implant surfaces can be divided into four groups: minimally rough (Sa between 0.5 and 1.0 µm), smooth (Sa < 0.5 µm), moderately rough (Sa between 1.0 and 2.0 µm), and rough (Sa > 2.0 µm). In general, slightly uneven surfaces get the best results [22].

1.10 Infection risk

The rejections of titanium implants on the grounds of bacterial infection and lack of bio-integration raise serious concerns about patient outcomes and significant healthcare costs [23]. Conventional Ti implants need to be improved to overcome these drawbacks, surface nano-engineering techniques and the creation of a new implant generation are seen as viable approaches. Medical implants are a particularly serious case because patients with weakened immune systems and/or compromised health can become infected. Furthermore, bacterial adherence preferentially attaches to implant materials. About 1% of all joint replacements actually result in the development of a prosthetic infection; however, this percentage rises significantly in cases of revision surgery [24]. In the field of dentistry, peri-implantitis has been noted in up to 14.4% of implants during the first five years; however, longer follow-up periods and after a first septic failure have been linked to a higher incidence of the condition [25]. Regarding bacteria, their filamentous proteinaceous

appendages can facilitate adherence to solid surfaces. Exopolymeric materials produced by bacteria aid in the development of biofilms and the ensuing long-term contamination of implanted surfaces [26]. A biofilm is a collection of various microorganisms that are permanently bonded to a surface and shielded by a self-produced polysaccharidic matrix (EPS) as previously mentioned. Organized bacteria are shielded by a biofilm from the effects of systemic pharmacological treatments as well as fluid shear stress. Additionally, it serves as a place to store materials and nutrients. Additionally, bacteria live in the organized and cooperative community of the biofilm-a polymeric protective structure that serves as a barrier between them and outside hardship-like they would in a city [27].

1.11 Factors effecting Biofilm formation

1.11.1 Surface roughness

Surface roughness plays a crucial role in biofilm formation on titanium implants. A study while testing effect of various factors on bacterial adhesion reveals that increased roughness leads to increased chances of bacterial attachment to implant surface. The surface topography analysis using the interferometer revealed that the turned surfaces had a surface roughness (Sa) of only 0.1 µm, indicating extreme smoothness. The blasted surfaces, on the other hand, had a moderate level of roughness, measuring 1.4 µm. The density of surface peaks (Sds) on both surfaces was similar, at about 150,000 summits per µm². However, the blasted surfaces had a significantly higher surface developed ratio (Sdr) at 58% ± 9.2 than the turned surfaces (2.8% ± 0.2). Even though the peak densities are similar, the difference in Sdr can be attributed to the blasted surface's increased roughness. As a result, on the blasted surfaces, there was 1.5 times more surface area available for bacterial adhesion than on the smooth turned surfaces [28].

1.11.2 Surface chemistry

Surface chemistry is critical in understanding how materials interact with their surroundings, particularly in medical applications such as titanium implants. The surface chemistry of the implant can be altered to improve its performance, particularly in terms of bacterial colonization and biofilm formation. For example, coating titanium implants with silver nanoparticles (AgNPs) significantly alters the surface and imparts strong antibacterial properties. These nanoparticles release silver ions, which disrupt bacterial cell membranes and metabolic processes, preventing

bacteria from adhering to the implant surface and forming biofilms. This modification not only reduces the risk of infection, but it also improves the implant's durability and biocompatibility.

Studies have shown that surface-treated implants can reduce biofilm formation by up to 96% compared to untreated surfaces. As a result, surface chemistry is critical in developing advanced implant coatings that are both safe and effective in medical applications [29].

1.12 Silver Nanoparticles and their Antimicrobial Activity

Regular cleaning and disinfection should be used to prevent the formation of biofilms, but some microorganisms can persist and occasionally form a biofilm for a variety of reasons. Many studies have been conducted to create new and more efficient methods of preventing the formation of biofilms. Some of these methods include choosing surface materials that prevent microbe attachment, altering the physiochemical properties of the surfaces, or adding antimicrobial products directly into the surface materials. Nanotechnology is opening up new possibilities for creating antimicrobial surfaces and better, more potent disinfectants and biocides [30]. Silver nanoparticles have excellent antimicrobial properties. The physical and chemical characteristics of Ag NPs, such as their size, shape, and surface charge, can significantly impact their antimicrobial activity due to their intricate antimicrobial mechanism. The constant release of silver ions from silver nanoparticles raises the possibility of a microbe-killing mechanism. Because of their stronger electrostatic attraction to sulfur proteins and their closer relationship to them, silver ions have no trouble adhering to the cytoplasmic membrane and cell wall [31]. In addition, the bacterial envelope is broken up because the silver ion attachment to the cytoplasmic membrane or cell wall increases the permeability of the cell, which in turn causes disruption of the cell. Reactive oxygen species are produced when cells absorb free silver ions, which deactivate respiratory enzymes and stop the synthesis of adenosine triphosphate. The main species that triggers DNA modification and disruption of cell membranes is ROS. Phosphate and sulfur are necessary elements in DNA. Nevertheless, AgNPs' interactions with phosphorus and sulfur in DNA can interfere with cell division and DNA replication, or even cause bacteria to die. Because silver ions can prevent protein synthesis, the ribosomes can occasionally become denatured in the cytoplasm [32].
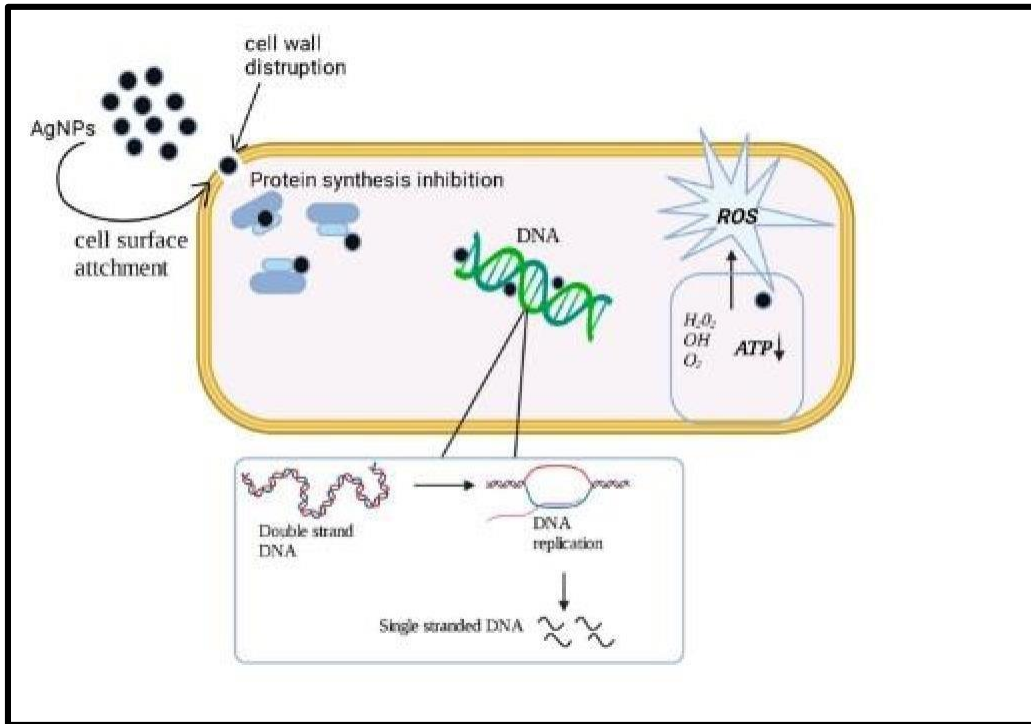
Figure 1.3. Mode of action of silver nanoparticles against bacteria, Silver nanoparticles penetrate the cell wall of bacteria and enter into the bacterial cell, releasing reactive oxygen species (ROS) which directly interact with the bacterial genome and disrupt activities of the cell, in return killing microorganisms.

CHAPTER 2: LITERATURE REVIEW

2.1 Polydopamine and Silver Nanoparticles for Antibacterial Coating

Biofilm production makes implants and medical equipment susceptible to bacterial infections. In one work, titanium alloy surfaces were coated with silver nanoparticles that were produced on polydopamine (PDA) particles. Using a variety of microscopy and spectroscopy techniques, the changed surface was able to demonstrate a decrease in surface roughness as well as an 85.78% and 96.14% efficacious resistance against Staphylococcus aureus and Escherichia coli, respectively. This technique presents a viable means of averting bacterial infections on medical equipment [33].

2.2 Silver Doping in Titanium Oxides for Antibacterial Enhancements

Because of its natural oxide layer, titanium, despite being frequently used in medicine, does not have the best bacterial resistance. Titanium oxides can be anodized to improve their characteristics, and the addition of silver has been demonstrated to increase photo catalytic activity (PCA) for improved bacterial resistance. This work investigated three different anodisation techniques with silver doping. The surface features such as topography and crystallinity did not change significantly, but improved PCA was observed in the silver-doped oxides that were obtained using sulphuric acid anodisation. All oxides exhibited a reduction in Staphylococcus aureus attachment under UVA light; however, the phosphorus-doped mixed-phase oxide exhibited the greatest reduction, indicating its superior antibacterial capabilities, due to its increased silver absorption [33].

2.3 Diversified Ion plating for Silver Implantation in Titanium surface

Another study examines the antibacterial properties of silver atoms implanted into titanium surfaces via Diversified Ion Plating at low energies (2 keV and 4 keV). Wettability, energy-dispersive spectroscopy, and profilometry were employed to evaluate the silver content of titanium. The quantity and depth of silver were precisely measured using Monte Carlo simulations and Rutherford Backscattering Spectrometry. Tests using Staphylococcus aureus (ATCC 12600) bacteria revealed that silver coated titanium surface were superior to pure titanium in terms of their ability to inhibit the growth of germs. This was particularly true at 4 keV, where prolonged silver release and deeper implantation were achievable. These results suggest that affordable antibacterial implant materials may be developed [34].

2.4 Antimicrobial Peptide and Silver Nitride coating for Titanium

Surface colonization and posterior infection by Staphylococcus aureus may compromise the success of titanium implantation. Various approaches have been studied to enhance titanium's antibacterial properties in order to prevent this problem. In this study, titanium surfaces were treated with two antibacterial agents: silver nanoparticles and a multifunctional antimicrobial peptide. The optimization of the modification of the nanoparticle density on titanium ($\approx 32.1 \pm 9.4$ nm) was achieved by means of a two-step functionalization approach that employed surface salinization. With both agents, a sequential functionalization was accomplished. The bactericidal qualities of each coating agent were assessed both alone and collectively. The outcomes demonstrate that all coated surfaces can experience a decrease in bacteria after 4 hours of incubation. However, the antimicrobial peptide coating alone proved to be more effective against Staphylococcus aureus after a 24-hour incubation period than either silver nanoparticles alone or in combination. Every coating that was tested did not cause any harm to eukaryotic cells [35].

2.4 TIO2 Nanotubes combined with Silver and reduced Grapheme Oxide

The biocompatibility of titanium alloys used in implants is improved by TiO2 nanotubes (NTs). In this work, reduced grapheme oxide (rGO) and silver nanoparticles (AgNP) were coated onto the nanotube surfaces after TiO2 NTs were produced on Ti6Al4V-ELI via anodic oxidation. According to the findings, TiO2 NT-AgNP enhanced antibacterial activity, however TiO2 NT-rGO postponed the formation of bacterial biofilms without harming the bacteria. These results point to potential methods for preventing implant-related infections: TiO2 NT-AgNP may lessen bacterial attachment, while TiO2 NT-rGO may aid in preventing biofilm formation [36].

2.5 Silver loaded coatings with controlled Ag Ion release

Using periodic array architectures, Ag-loaded coatings with improved osteogenic and antibacterial characteristics were created for implants. Through manipulation of the hydroxyapatite (HA) content and etching spacing, the controlled release of silver ions was accomplished. With this method, bacterial growth can be successfully inhibited while cytotoxicity is minimized. Silver ions can be released at two different rates: quickly at first and more slowly afterwards. This technique

presents a viable substitute for implants that necessitate both antimicrobial and osteogenic properties [37].

2.6 TIO2 and Silver Nanoparticle coating on 316L Stainless steel

A promising way to stop corrosion is to grow TiO2 films on the metal implants surface, which extend the prosthesis into the bone and increase biocompatibility. Moreover, the antimicrobial properties of silver nanoparticles are well known. In this work, we propose to combine the antibacterial activity of metallic silver nanoparticles with the biocompatible properties of TiO2 coatings by synthesizing the nanoparticles as thin films on 316 L stainless steel. These coatings were created using the inexpensive and versatile synthetic process known as sol-gel. The corrosion resistance of 316 L steel samples coated with these films was evaluated using the linear polarization technique using a simulated body fluid (SBF) solution at 37 °C and a pH of 7.25 [38].

2.7 Silver Nanostars synthesis and structural properties

To meet demand, different sizes and shapes of silver nanoparticles (AgNPs) have been produced using different synthesis techniques. According to Lois au et al., a particular technique is needed to produce AgNPs in the desired shapes, such as nanospheres, nanowires, nanocubes, and so forth. They also summarized all feasible techniques, including the polyol process and chemical reduction method, to accomplish this. Nevertheless, AgNSs, or silver in the form of a nanostar, is one of the intriguing nanostructures because it has the lowest plasmonic losses in the UV-visible spectrum and a very strong plasmonic effect in comparison to other shapes. This means that it theoretically should improve the signal of the sensor, particularly for plasmonic bio sensing [39]. Furthermore, AgNs synthesized are less expensive than Au nanoparticles (AuNPs).

2.8 SERS Detection of Ciprofloxacin with Ag Nanostars

The overuse of antibiotics in aquaculture and livestock has made it more crucial than ever to find antibiotic residues in food. This work emphasizes the application of surface-enhanced Raman scattering (SERS) to the antibiotic ciprofloxacin trace detection. Because of the synergy between AgNSs and aluminium foil, the SERS substrate, which is composed of AgNSs on foil, greatly increased Raman signals. The silver nitrate-reducing AgNSs have pointed arms that radiate from a central core. With a detection limit of 0.23 ppb, this configuration allowed the detection of ciprofloxacin at very low concentrations [40].

2.9 Silver Nanostars and their Antimicrobial properties

Antimicrobial surface engineering and the development of better and more potent disinfectants and biocides are now possible thanks to nanotechnology. Well-known broad-spectrum antimicrobial agents are silver nanoparticles. It is thought that their potent antibacterial activity stems from multiple mechanisms working together in different bacterial targets simultaneously. Tang and Zheng [41] claim that three mechanisms—direct binding, silver ion release, and the production of reactive oxidative species—allow silver nanoparticles to influence DNA, membrane proteins, and cell membranes. It is well recognized that the degree of antibacterial activity is influenced by both chemical and physical characteristics, including stability, size, shape, and surface chemistry [42]. Although silver atoms (Ag0) make up silver nanoparticles, these atoms can be changed into silver cations (Ag+), which are subsequently released from the particle's surface into the medium (usually aqueous). The rate at which this conversion occurs can vary from an instantaneous reaction to an ion-by-ion, layer-by-layer release, depending on the redox conditions of the medium. While spherical silver nanoparticles are the most prevalent, other shapes, such as stars, rods, platelets, and cubes, have also been created [43]. Silver nanostars (AgNSs), have a core from which several arms extend. The length of these arms can be changed by adjusting the reduction time and reagent concentration. When compared to spherical nanoparticles, star-shaped nanoparticles have a higher surface area to volume ratio. The study's description of AgNSs revealed that coating surfaces which turn strongly biocidal shows more promise for application than suspension for antimicrobial purposes. When it comes to optimizing or engineering silver- based surfaces for use in the biomedical and industrial domains, AgNSs hold great potential as a starting point [44].

2.10 Influence of shape on Antibacterial activity

The numerous benefits of silver nanoparticles (Ag NPs), such as their optical, electrical, antibacterial, and catalytic capabilities, make them useful in a broad range of applications. The physical and chemical characteristics of Ag NPs, such as their size, shape, and surface charge, can significantly impact their antimicrobial activity due to their intricate antimicrobial mechanism [45]. The OD growth curve test and the paper disk method were used to confirm the antimicrobial activity of the Ag NPs based on their morphology.

2.11 Influence of size on Antibacterial activity

The silver nanoparticles had a restricted size distribution and spherical (7 and 29 nm) and pseudo spherical (89 nm) forms, according to experiments using transmission electron microscopy (TEM). It was discovered that when the size of the nanoparticles decreases, their antibacterial activity increases. Results show that nanoparticles with 7nm size have greatest antibacterial activity and those with 89nm size has smaller antibacterial as compared to others [46].

2.12 Influence of Nanoparticle concentration on Antibacterial activity

The antibacterial activity of silver nanoparticles (AgNPs) is influenced by their quantitative significance. Because of the restricted release of silver ions, which interact with bacterial cell membranes, proteins, and DNA, and impair their functionality, AgNPs can show moderate antibacterial effects at low concentrations. Because more silver ions are released, which damages bacterial cells more severely, antibacterial activity usually rises with amount. Beyond a certain point, though, further addition is probably not going to make a big difference in terms of antibacterial activity and might even be harmful to human cells. As a result, it's critical to maximize AgNP concentrations in order to preserve a balance between minimal tissue damage and efficient bacterial inhibition [47].

2.13 Coating of Titanium Implants with Silver Nanostars

Since silver nanoparticles (AgNPs) have strong antibacterial qualities and are crucial in preventing implant-related infections, AgNP coatings on titanium implants are becoming more and more popular. Silver nanoparticles are effectively coated onto the titanium surface using a variety of techniques, guaranteeing their uniform distribution, stability, and long-term functionality. The objective of these techniques is to preserve the mechanical properties of titanium implants while enhancing their bioactivity. Researchers can regulate the release of silver ions, which directly impacts the implants' biocompatibility and sterilizing capabilities, by selecting the right plating technique. There are many techniques for coating of different nanoparticles on titanium implants [48].

Because titanium implants have excellent mechanical qualities and are biocompatible, they are frequently utilized in orthopedic and dental procedures. But these implants are vulnerable to bacterial infections, particularly when the bacteria take the form of biofilms, which can result in major side effects like implant failure, protracted healing, and the need for additional surgeries.

Present implant coatings frequently fall short of the required level of biocompatibility while failing to offer sustained antibacterial protection. Novel approaches are needed to address the ongoing problems with orthopedic and dental implant infection prevention. By creating silver nanoparticles and applying them as a biomimetic coating to titanium implants, this study tackles this important problem. The goal of this research is to determine whether these novel coatings have the potential to improve surface characteristics, lower biofilm formation, and greatly increase antibacterial effects—all of which could have a bearing on medical and dental applications can offer implant solutions that are more dependable and safe.

2.14 Aims and Objectives

- To use a reduction method with NaOH as the reducing agent to create star-shaped silver nanoparticles.

- Investigate various coating methods to guarantee uniform and long-lasting AgNP deposition onto titanium implant surfaces, thereby augmenting the antimicrobial characteristics.

- Assess the ability of AgNP-coated implants to inhibit bacterial growth and biofilm formation in order to determine how effective they are at preventing implant-related infections.

- Utilizing advanced surface analysis techniques, evaluate the AgNP-coated titanium implant surfaces' morphology and topography.

CHAPTER 3: MATERIALS AND METHODOLOGY

In this work, we investigated the antibacterial properties of titanium implants coated with silver nanostars using a comprehensive experimental design. First, a chemical synthesis method was used to create silver nanostars. Then, a variety of techniques, such as scanning electron microscopy (SEM), X-ray diffraction (XRD), RAMAN spectroscopy, Fourier transform infrared spectroscopy (FTIR), and UV visible spectroscopy, were used to characterize them. Following these characterization methods, the nanostars were biomimetically coated on a grade 5 titanium disc (Ti-6Al-4V). The titanium disc was first heated and then subjected to an alkaline process before being submerged in simulated body fluid (SBF) to facilitate the coating of calcium phosphate and the suspension of nanoparticles. Dip coating was the method of coating employed. Following coating, the disc underwent additional characterization, and its antibacterial efficacy was assessed.
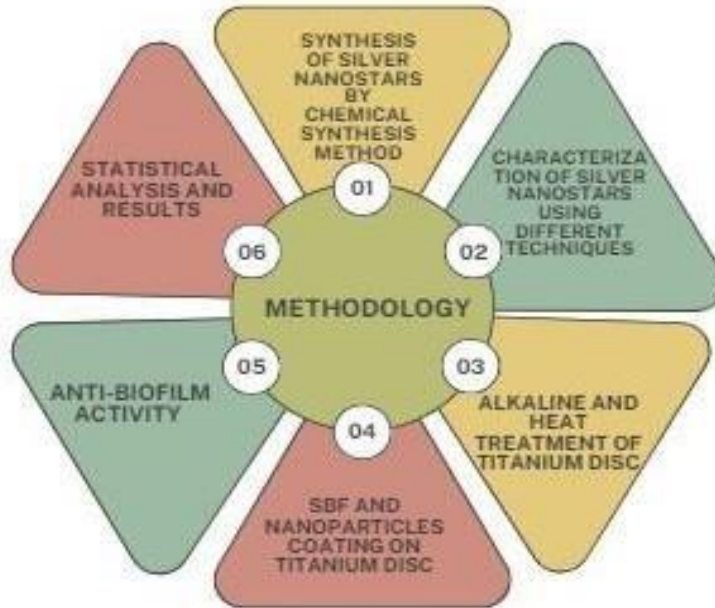
Figure.3.1 Experimental timeline, the figure illustrates the methodology of evaluating antibiofilm activity of silver nanostars coated titanium implants

3.1. Materials

- Silver nitrate($AgNO_3$)
- Polyvinylpyrrolidone (PVP)
- Poly ethylene glycol(PEG)
- Sodium hydroxide(NaOH)
- Distilled Water
- Ethanol
- Simulated body fluids (SBF)
- Sodium Chloride (NaCl)
- Magnesium chloride hexahydrate ($MgCl_2 \cdot 6H_2O$)
- Calcium chloride dehydrate ($CaCl_2 \cdot 2H_2O$)
- Disodium hydrogen phosphate dihydrate ($Na_2HPO_4 \cdot 2H_2O$)
- Sodium bicarbonate ($NaHCO_3$)
- Tryptic soy agar(TSA)
- Tryptic soy broth(TSB)

3.2 Chemical synthesis of Silver Nanostars

Using NaOH ($4 \times 10{-}2$ M) as a reducing agent, reduction of the silver precursor salt ($4 \times 10{-}3$ M) was carried out in a solvent mixture of ethylene glycol (11 g) and PVP (0.053 g). Silver nitrate was first added to the solvent mixture, which was heated to 190 °C for 30 minutes. Next, the precise quantity of NaOH was added. The solution turns into milk tea color upon the addition of NaOH indicating the synthesis of Ag(0) nanomaterial stabilized in the mixture of PVP and ethylene glycol [49]. After that, the mixture is agitated for nearly five minutes with a magnetic stirrer, revealing minuscule. After adding the solution in beaker to the falcon tubes, the mixture is centrifuged for 10 minutes at 6000 rpm to form a pellet. Following the removal of the supernatant, the solution is mixed in a vortex mixer with distilled water before being centrifuged once more. This process is repeated two or three times to remove impurities. After that, the extra water is

disposed of once more, to obtain the nanoparticles in the form of fine powder, the pellet is stored in a petri plate and placed in oven for 48 hours at 50°C.

Figure.3.2. Silver nanostars in fine powder form

3.3 Characterization of silver nanostars

A thorough analysis of silver nanostars is required to comprehend all of their characteristics, particularly in light of their possible uses in the biomedical industry. To see the morphology and surface structure of nanostars and learn more about their star shape, scanning electron microscopy, or SEM, is utilized. In order to ascertain the optical behavior of nanostars, UV-vis spectroscopy is utilized to investigate their plasmonic properties. Whereas Fourier transform infrared spectroscopy (FTIR) locates functional groups on the surface of the nanostar, Raman spectroscopy offers details on chemical structure and molecular vibrations. To verify the phase and purity of nanostars, X-ray diffraction (XRD) is for analyzing their crystalline structure. To investigate the surface charge of the nanostars, which influences their stability and interactions in various environments, the zeta potential is also measured. When combined, these diagnostic methods allow for a thorough comprehension of the chemical, optical, and structural characteristics of silver nanostars.

3.4 Scanning Electron Microscopy

A strong imaging method for producing incredibly detailed three-dimensional images of a sample's surface is scanning electron microscopy (SEM). With a high zoom and depth of field, this method produces detailed images by scanning a sample with a focused electron beam and analyzing the secondary electrons that are emitted. For examining the morphology, topography, and chemistry of materials at the nanoscale, SEM is indispensable. For SEM, the sample can either be given in the form of powder or suspension in which we add 0.001 grams nanoparticles sample in 10 ml of distilled water. Mostly it is given in the form of suspension because it allows better dispersion of nanoparticles and prevent them from agglomerating. The suspension is placed on a glass slide, dried and coated with a conductive layer such as gold to prevent buildup of electric charge on sample surface and it improves contrast and produce a better image. Sample is then placed in vacuum chamber that prevent electron scattering by air molecules, a beam of electron falls on sample surface which interact with sample and produce secondary and backscattered electrons. These scattered electrons are collected by a detector and an image is created that can be seen on a computer screen.The machine used for SEM of my samples was named as Jeol JAM-6490A.

3.5 X-ray Diffraction

One method for determining and examining a material's crystal structure is X-ray diffraction (XRD). This method measures the angle and intensity of the scattered rays of X-rays that are focused on a sample. The resulting diffraction pattern allows for a detailed characterization of the state, structure, and crystallinity of the material by revealing the arrangement of atoms within the crystal lattice. The sample for XRD is usually in the form of powder which give accurate results. The sample is placed on a sample holder and X-rays fall on it through an X-ray source and when these X-rays come in contact with crystal lattice, they are diffracted at specific angles. Then these diffracted rays are detected by a detector which analyze these rays and produce a diffraction spectrum.

3.6 RAMAN Spectroscopy

A method for determining molecular vibrations and examining a sample's chemical makeup is Raman spectroscopy. This aid in describing the molecular structure, chemical bonds, and various phases of the material. For RAMAN the sample was given in the form of powder, which was

placed in the stage or sample holder and a beam of monochromatic light is directed towards the sample which interacts with the molecular vibrations of the sample and is scattered in different directions and experience a shift in wavelength which is known as "RAMAN shift" This scattered light was then collected by a detector and RAMAN spectrophotometer measures the frequency shift between the incident light and the scattered light .The frequency shift produce a spectrum which tells us about the vibrational mode of the molecules in sample.

3.7 UV visible Spectroscopy

An analytical method called UV-visible spectroscopy calculates how much ultraviolet and visible light a sample absorbs. The analysis of organic compounds, transition metal complexes, and other substances is frequently done using this technique. The sample is in the form of liquid and placed in a 96 well plate, a transparent container with 96 small compartments is placed in a horizontal section in UV spectrophotometer. A light source mostly deuterium lamp (for UV light) or tungsten lamp (for visible light) produces light that passes through a monochromator that splits the light in different wavelengths. When the light falls on the sample, some of the light is absorbed by sample while some continues to pass through. Then the machine measures the amount of light that passes through the sample and compares it with the light that went in. This produces a spectrum that shows what part of light was absorbed, and tells us about the composition and quantity of sample.

Figure.3 3. Microplate reader

3.8 Fourier Transform Infrared (FTIR) Spectrophotometer

(FTIR) spectroscopy is used to determine and examine a sample's molecular makeup. The material's functional groups and chemical bonds are identified by the resulting spectrum, which makes it possible to ascertain the material's molecular structure and composition. The sample was given in the form of fine powder, which was placed in a sample holder, and then infrared light was passes through the sample to determine the amount of light absorbed at various wavelengths. The spectrophotometer measures transmitted light and records absorption data that creates an infrared spectrum which provide information about the chemical bonds of the sample.

3.9 Zeta Potential Analyzer

The amount of electrical charge on the surface of particles in colloidal suspensions is measured by zeta potential. It displays the strength of attraction or repulsion between particles, which has an impact on the suspension's stability. While a low zeta potential can lead to particles sticking together and lacking stability, a high zeta potential indicates good stability. This characteristic is crucial for comprehending and managing the behavior of emulsions, colloidal systems, and nanoparticles. The sample for zeta is in liquid form and is placed in a cuvette designed especially for zeta potential analyzer. An electric field is applied to the sample and the particles in the sample start moving towards the electrodes, then the speed of the particles was measured. Faster movement means greater charge which tells us that more stable the sample is. And if the zeta potential is smaller it means that the samples have weak electric charge that reduce the repulsion between them and increases the chances of aggregation, and in turn reduce the stability of the sample.

3.10 Alkaline and heat treatment of Titanium Discs

For alkaline treatment, the discs were dipped in a 5M NaOH aqueous solution at 80°C in lab drying oven for 72 hours, after 3 days the discs were washed with distilled water and air dried at 40°C for 24 hours. After alkali treatment, the samples were heated at 600°C for 1 hour in an electrical furnace. The discs were then observed under optical microscope.

3.11 Biomimetic coating on Titanium Disc

The chemical reagents NaCl (4.8 g), $MgCl_2 \cdot 6H_2O$ (0.18 g), $CaCl_2 \cdot 2H_2O$ (0.22 g), $Na_2HPO_4 \cdot 2H_2O$

(0.10 g), and NaHCO3 (0.21 g) were dissolved in 120 ml of distilled water and stirred for 10 to 15 minutes to create the SBF solution. After preparing SBF solution, it was poured into two different petri plates along with nanoparticle solution (0.01 g powder in 10 ml of distilled water). The discs were dipped in both petri plates and were labelled as group 1 and group 2. For group 1, the disk will remain in SBF for 7 days, and for group 2 the disc will be in solution for 14 days, and both the solutions were refreshed every 48 hours [50].

Figure.3.4. Titanium disc immersed in SBF*AgNSs solution

3.12 Measuring Contact Angle of Treated and Untreated Discs

Contact angle is the angle formed between tangent of liquid droplet and the solid surface on which the droplets rests. It measures how well a liquid spreads on a surface.

- If contact angle is greater than 90°, it means that the liquid does not spread well on solid surface i.e. the surface is hydrophobic.

- If contact angle is smaller than 90°, it means that the liquid spread well on the surface, i.e surface is hydrophilic.

Contact angle was measured in order to check the surface wettability of treated and untreated disc, which influence properties like cell attachment and bacterial adhesion and to evaluate if silver nanostars coating can reduce the bacterial attachment or not . Osseo-integration and biocompatibility of titanium disc can also be determined by measuring the contact angle.

Contact angle is measured using a device called "contact angle goniometer". In this process, both the discs were taken and a drop of liquid typically water was taken and placed on the surface of titanium discs using a micropipette. A high resolution camera is used to capture side view of droplet as it sits on the surface of disc, then a software is used to measure the angle between tangent to the droplet and solid surface.by analyzing the angle we can determine the wettability of the solid surface.

3.13 Antibiofilm activity

Prepare a bacterial culture of Staphylococcus aureus in 5 ml of nutrient-rich broth (TSB) and incubate it overnight at 37°C to test the antibiofilm activity of silver nanostars. The bacterial cultures should be diluted (1:100) and then added to four separate wells of a 96-well microplate. Next, include four distinct solutions in it. In the first, is the 7 days coated disc dipped overnight in broth ,in the second one is the 14 days coated disc dipped overnight in broth in the third one is ethanol which is used as a negative control group; and in the fourth, there is only nutritional broth used as a positive control. Once the well plate has been filled with all of these solutions, incubate it for 24 hours at 37°C to promote bacterial growth. The biofilm will stay attached to the well plate even after you carefully remove the liquid from the plates after a 24-hour period. Now fill each well with 0.1% weight by volume of crystal violet dye, and let it sit at room temperature for 15 minutes to allow the dye to attach to the biofilm.

To guarantee that only the biofilm left after nanoparticle treatment will be stained, carefully wash the wells with distilled water to remove any excess stain, then allow them to dry at room temperature. At 630 nm, measure the absorbance of each well. The absorbance values will show how much biofilm is in each well, and the well that will turn crystal violet will have biofilm in it. Compute the percentage of biofilm inhibition using a formula by comparing the absorbance values of both nanoparticle concentrations with the control group [51].

$$Inhibition \% = (C-B)-(T-B) / C-B \times 100$$

CHAPTER 4: RESULTS AND DISCUSSIONS

After synthesis of silver nanostars, they were characterized by different testing techniques that indicates that the nanoparticles are of specific desired size and shape.

4.1.1 Ultravoilet spectrum

Silver nanoparticles usually show ultraviolet absorption around 350 to 450 nanometer. The spectrum below is UV visible spectrum of silver nanostars and is measured using MULTISKAN SKY micro plate reader in which UV of multiple samples at a time can be calculated, In this spectrum silver nanostars are showing peak at 407 nm . The red line is indicating AgNSs and blue line is indicating distilled water added as blank. Because the light causes specific vibrations in the surface electrons of silver nanostars, the light is absorbed at around 400 nanometers. This process, known as localized surface Plasmon resonance, is caused by their distinct star-like shape (LSPR).
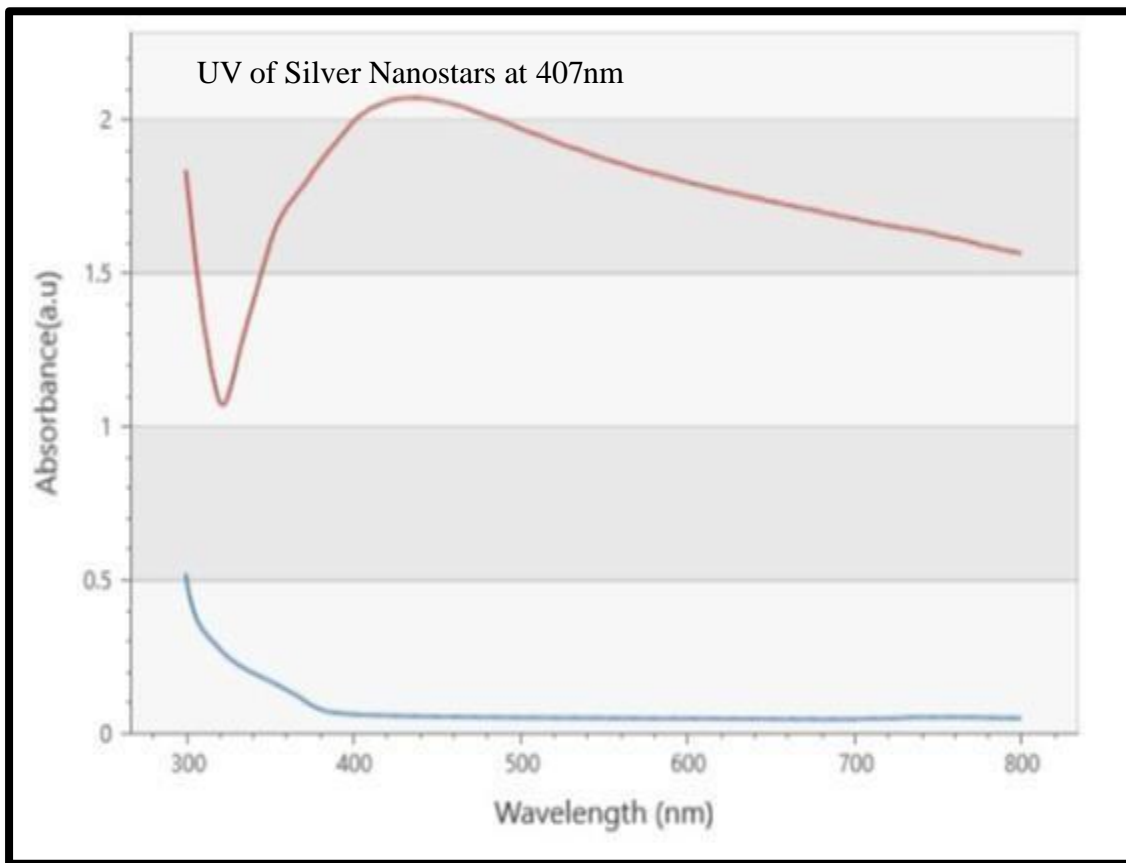
Figure 4.1. Silver Nanostars showing absorption at 407 nm wavelength due to their localized surface resonance

4.1.2 Zeta Potential

The average zeta potential of my silver nanostars is -26 mV, indicating excellent colloidal stability. This negative value effectively lowers the risk of agglomeration by indicating a strong electrical tension between individual particles. The outcome is that the nanostars are evenly distributed throughout the solution, preserving their structural integrity and guaranteeing their consistent behavior across a range of applications. Maintaining the distinctive characteristics of nanostars is crucial for preserving their efficacy and dependability in both experimental and real-world settings.

Figure 4. 2. A graph showing zeta potential of silver nanostars at -26.6, which indicates that the nanostars have better stability.

The electrophoretic mobility (μ), zeta potential (ζ), and standard deviation (σ) of silver nanoparticles are displayed in the table below. The speed and direction of the nanostars under the electric field are indicated by the average electrophoretic mobility in the raw data, which is -2.07 μm.cm/V.s. Because the st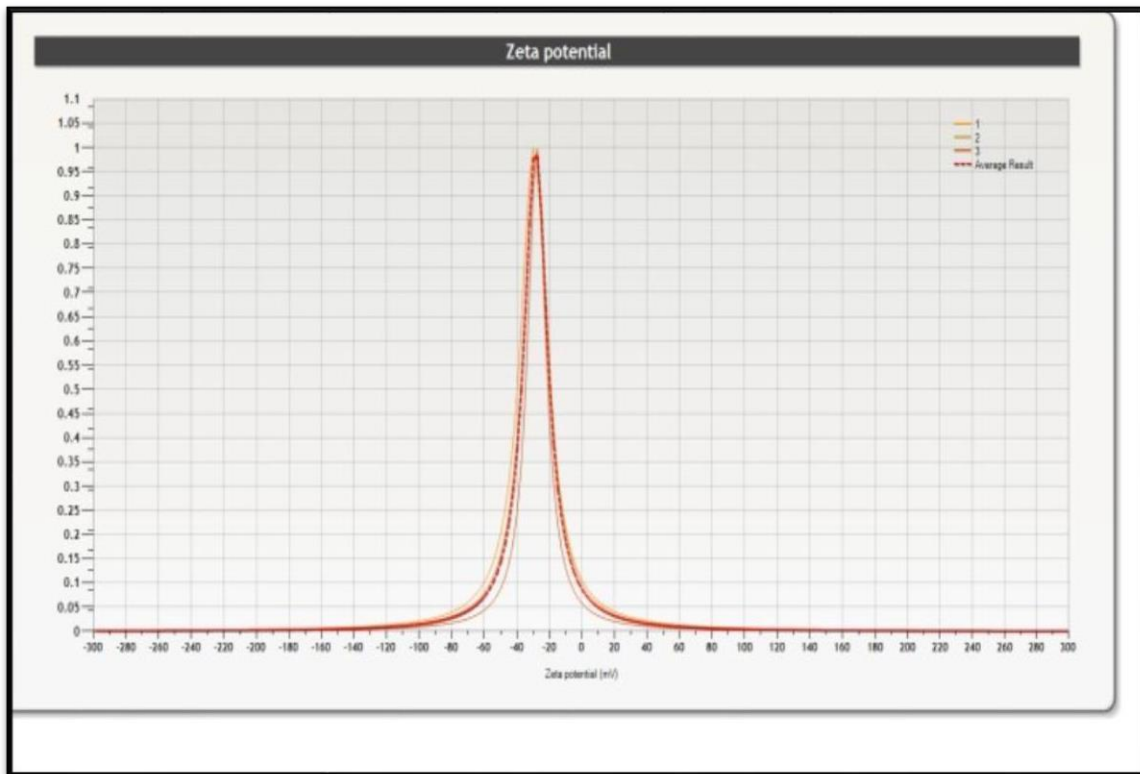rong electrical potential inhibits particle aggregation, the average zeta potential of -26.6 mV suggests a more negatively charged surface, which often implies good stability. The diversity in the measurements is reflected in the raw data's standard deviation of -2.22. The average electrophoretic mobility increases to 0.68 μm.cm/V.s and the zeta potential to 28.6 mV when the data are fitted, demonstrating that the technique was adjusted during analysis. A high zeta potential value nevertheless denotes stability in spite of this shift. The fitted data's standard deviation, which represents the variation in the adjusted measurements, is 8.79. Overall, the silver nanoparticles are probably stable in suspension solution based on the substantial value of zeta potential in both the raw and fitted data.

Values

#	Valid	Raw		Fit			
		μ (μm.cm/V.s)	ζ (mV)	μ (μm.cm/V.s)	σ	ζ (mV)	σ
Avg		-2.07	-26.6	-2.22	0.68	-28.6	8.79
1	☑	-2.13	-27.43	-2.3	-0.79	-29.57	-10.2
2	☑	-1.94	-24.93	-2.21	-0.72	-28.43	-9.3
3	☑	-2.13	-27.43	-2.16	-0.54	-27.78	-6.88

Figure 4.3. Figure shows Electrostatic stability, zeta potential and standard deviation of silver nanostars.

4.1.3 X-ray Diffraction

The XRD graph below displays multiple peaks at various angles, which correspond to the diffraction of the X-ray rays by particular crystal planes in the sample. These peaks are labeled with Miller indices, such as (200), (111), (220), and (311), which indicate the orientation of the planes within the crystal lattice. These peaks are caused by Bragg's law, which states that the more path difference between X-ray beams, the more powerful they are when combined. The sharpness and intensity of the peaks reveal details about the crystalline structure, purity, and domain size of the material; higher intensity peaks correspond to planes with higher density of atoms or electrons, which aid in the identification and understanding of the material.
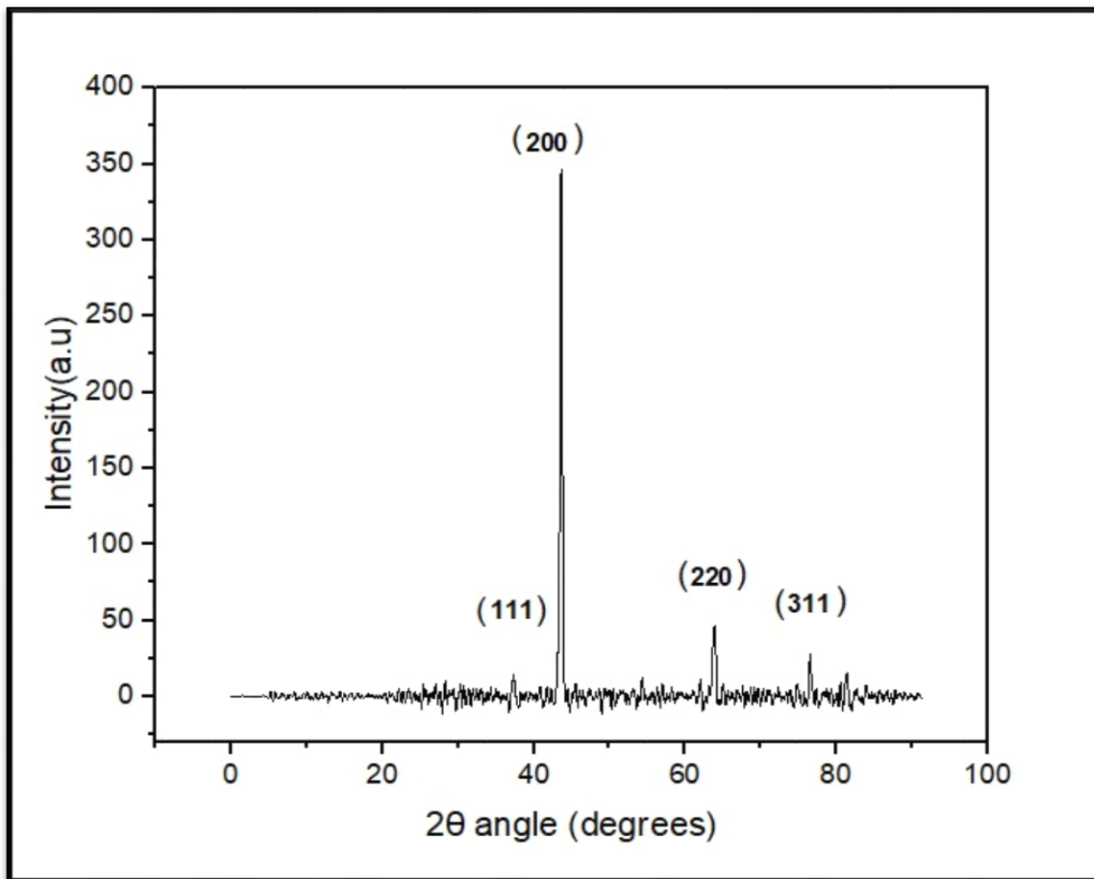

Figure 4. 4. XRD peaks of silver nanostars

XRD graph resembles the common diffraction patterns found in silver nanostars. Silver nanostars usually exhibit maxima on particular planes, this graph includes (111), (200), (220), and (311).

The face-centered cubic (FCC) crystalline structure of silver nanoparticles is represented by these peaks. These peaks suggest that the sample's crystalline structure most likely mimics that of silver nanostars.

4.1.4 Fourier Transform Infrared Spectroscopy

FTIR tells us about the individual component of a molecule or bonds present in the molecular structure that show vibrations at specific peaks in an FTIR spectrum. The peaks represents the following bonds present in PVP and PEG, which were used in synthesis of silver nanostars, AgNO3 don not show any peak in FTIR region because it is reduced during the synthesis process and NaOH itself is infrared inert and don not show any peak in IR region. The existence of these particular connections raises the possibility that different PVP and maybe PEG functional groups are interacting inside the artificial silver nanostars. Stabilizing chemicals like PVP, which aid in preventing aggregation and preserving the stability of the nanostars, are shown by the O-H and C=O stretching vibrations.
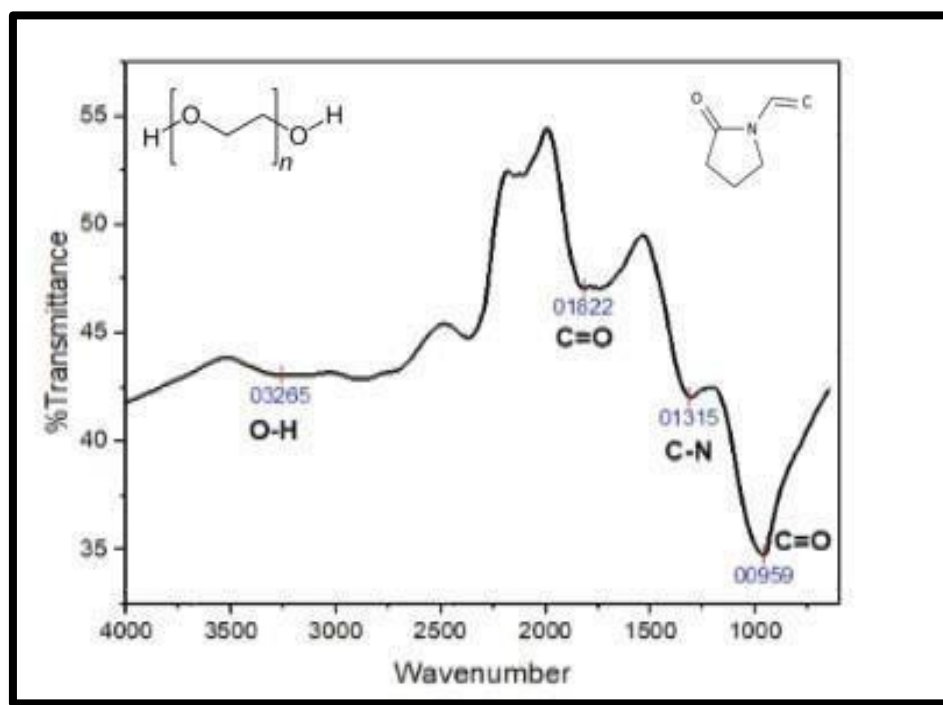

Figure 4.5. 3254 cm^{-1} indicates O-H stretching vibrations, 1822 cm^{-1} indicates C=O stretching, 1315 cm^{-1} for C-N stretching and 959 cm^{-1} is indicating C=O stretching present in both PVP and PEG.

4.1.5 Raman Spectroscopy

Vibrational, rotational and other low frequency modes in a system can be studied by Raman spectroscopy, it helps in understanding the structural and chemical composition of the material. The silver nanostars, which were made with PVP, PEG, NaOH, and AgNO3, exhibit multiple different peaks in the Raman spectroscopy data. The presence of a silver-nitrogen bond is indicated by the signal at 234 cm^{-1}, which may have resulted from contact with nitrogen-containing groups in PVP. The presence of a silver-oxygen bond is indicated by the signal at 480 cm^{-1}, which could be the result of interaction with residues in AgNO3 or oxygen-containing groups in PEG. The carbon-hydrogen bonds shown by the peaks at 690 and 730 cm^{-3} are typical of organic compounds like PVP and PEG. PVP's distinctive carbon-nitrogen bonds can be seen at the peak at 921 cm^{-1}. Lastly, carbon-carbon double bonds are visible at the peak at 1635 cm^{-3}; these bonds are probably found in the polymer backbone of PVP.
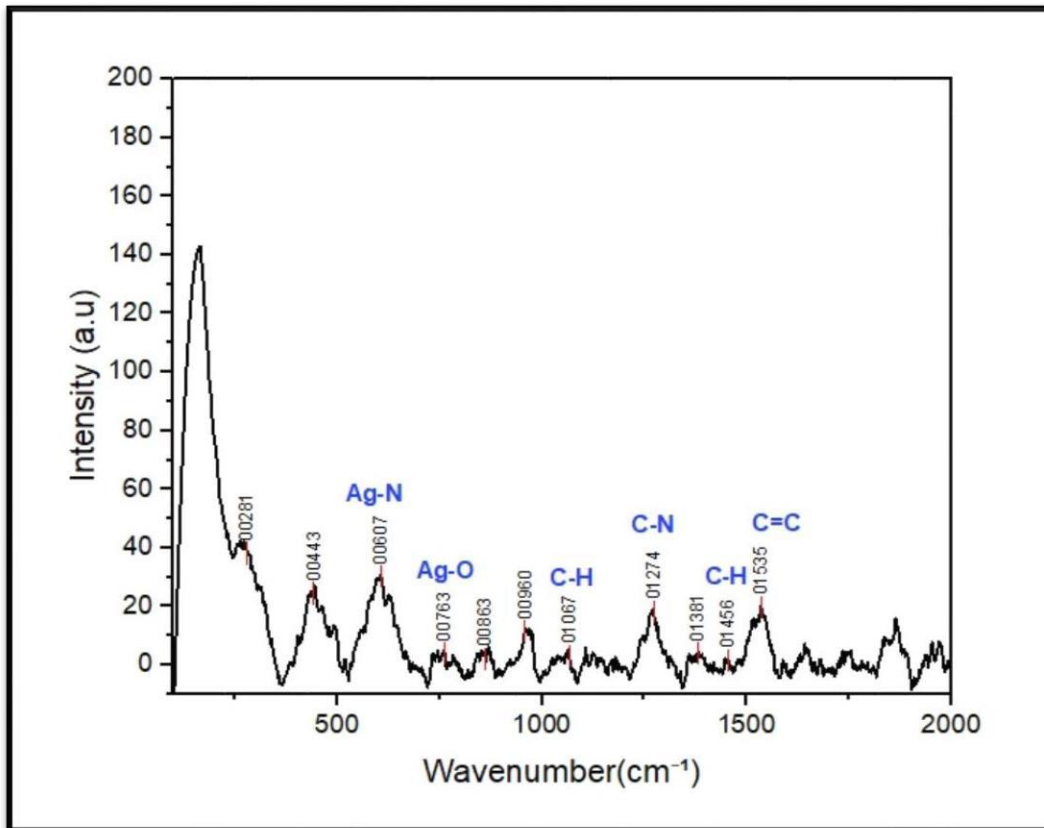
Figure 4.6. All these peaks showing different chemicals bonds present in silver nanostars individual components

4.1.6 Scanning Electron Microscopy

Due to its higher density, silver typically appears in SEM pictures as clusters of bright material against a darker background. This is how the structures look as given below. The asymmetrical aggregates point to the presence of many arms or protrusions, which are traits of nanostars. The brilliant, asymmetric clusters in the SEM image indicate that the manufacture of silver nanostars was effective, despite the limits. Some of SEM images are given below.
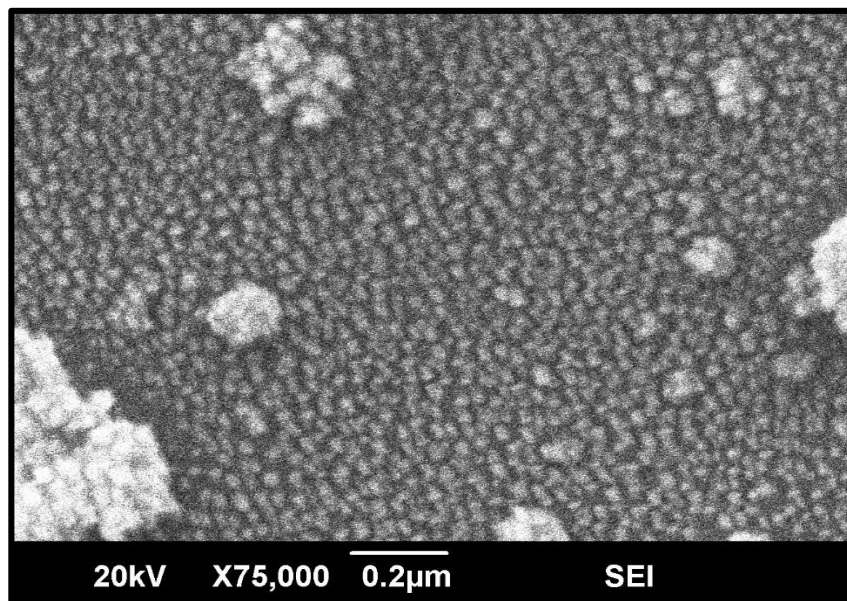
Figure 4.7. These SEM images are showing structure of silver nanostars at magnifications of 75,000 times, they are much zoomed pictures of silver nanoparticles that's why distinct nanostar like structures are not visible due to machines limitations. These nanoparticles have a different star like structure with main body having greater diameter than the arms which are having less diameter than main body.
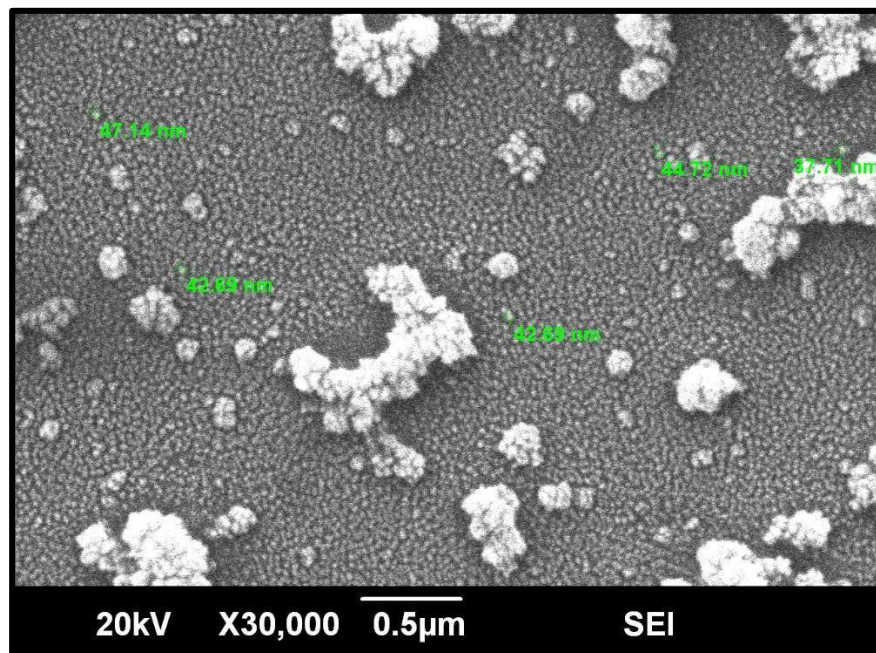
Figure 4.8. Silver nanostars with different sizes at magnification of 30,000 and 500nm scale.
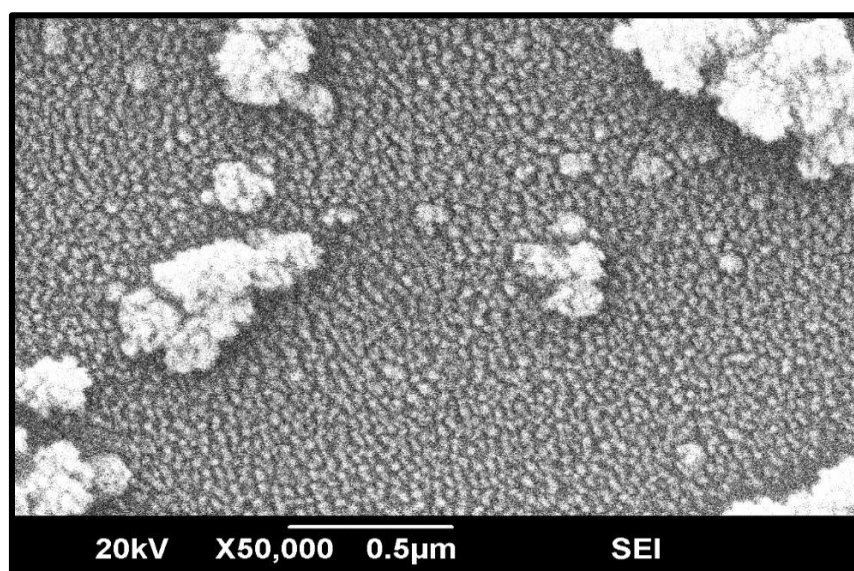
4.1.7 Size Analyzer

Size distribution of silver nanostars include a wide range of sizes from smallest to largest nanoparticles, the average size of nanoparticles was from 40 to 70 nm but this broad range of size was because of the formation of agglomerates that were of larger size but individual nanoparticles size was less than 70 nm .silver nanoparticles usually from agglomerates maybe due to weak forces of attraction between the particles or growth of smaller nanoparticles over the larger ones that leads to agglomeration. The graph shown in figure 4.9 below shows the size distribution of nanostars. This graph was obtained from size analyzer machine named HORIBA LA-920 ver.3.70 that give us cumulative distribution graph of sizes of AgNSs.
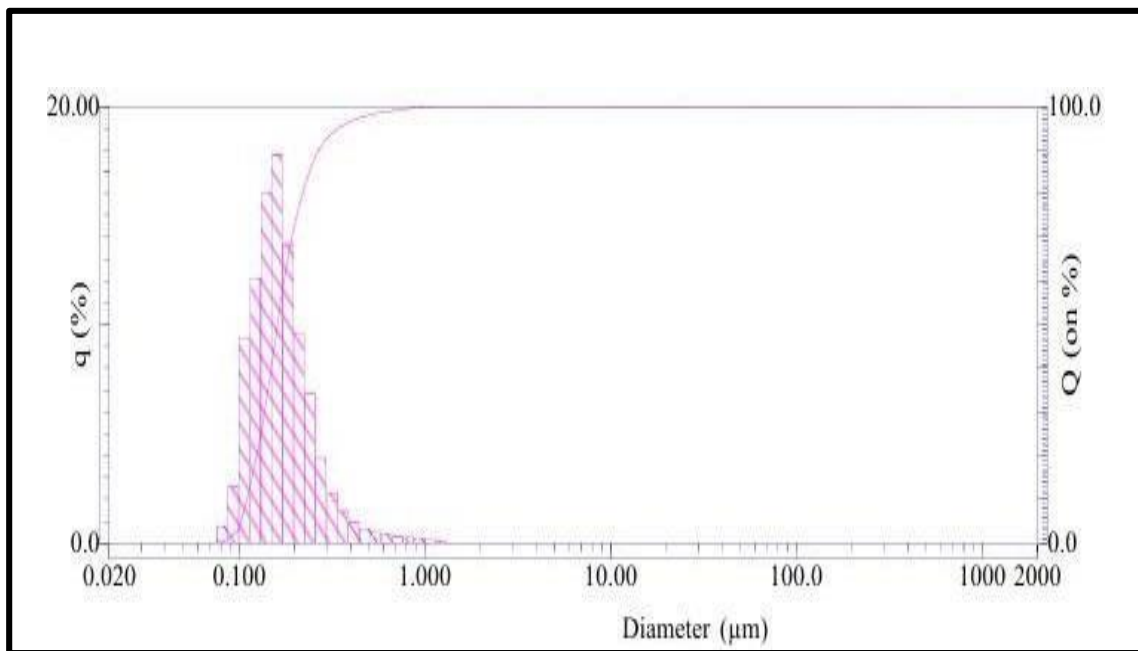
Figure 4. 9. Graph showing multiple sizes of star like silver nanoparticles.

The successful synthesis of silver nanostars has been confirmed by comprehensive characterization techniques. The clear peaks observed in the X-ray diffraction (XRD) pattern are consistent with the face-centered cubic (FCC) structure of silver, confirming the crystalline nature of the nanostars. Raman spectroscopy results show characteristic peaks with silver-nitrogen and silver-oxygen bonds as well as carbon-nitrogen and carbon-carbon double bonds, indicating interactions with capping agents such as PVP. Additionally, UV-vis spectroscopy shows a prominent absorption peak around 410 nm, consistent with the expected plasmonic resonance of silver nanostars. These results, together with consistent measurements of zeta potential and consistent particle size in transmission electron microscopy (TEM), confirm the successful formation and structural integrity of aggregated silver nanostars.

4.2. Alkaline And Heat Treatment
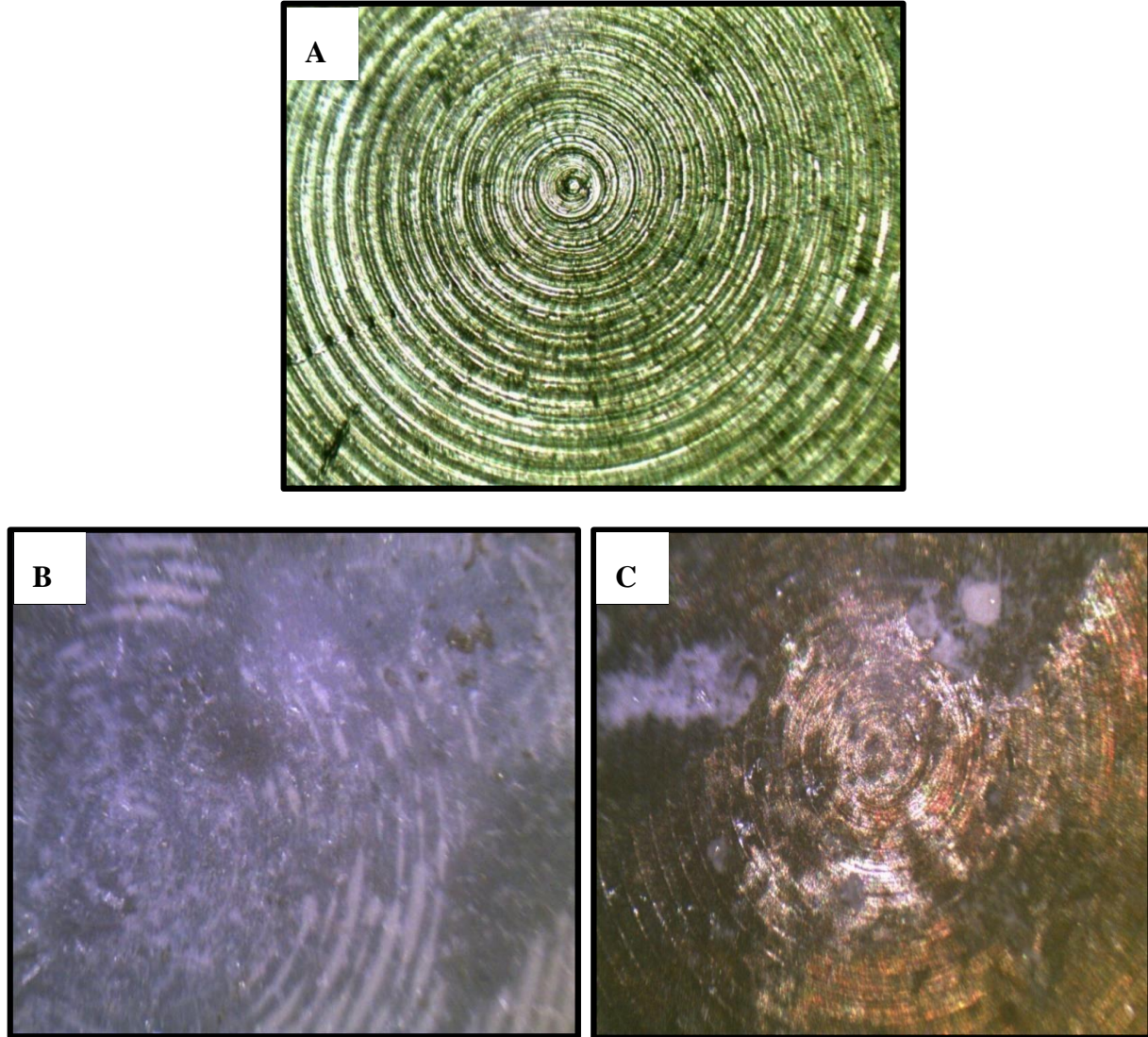
Figure 4.10. Titanium disc (A) without heat and alkaline treatment (B) And (C) showing images of titanium disc after alkaline and heat treatment. The white cloudy appearance occurs because of chemical reaction between NaOH and titanium surface especially under heat treatment

4.3 Coating on Titanium Disc

After coating the titanium discs with a solution containing SBF and nanoparticles, they were put on petri dishes and left there for seven and fourteen days, with the solution being replaced every 48 hours. Subsequently, the discs were examined using a scanning electron microscope to determine the success of the coating process.

4.3.1. Untreated Disc The untreated disc is not showing any particles nanoparticles on it, it is like a plane disc.
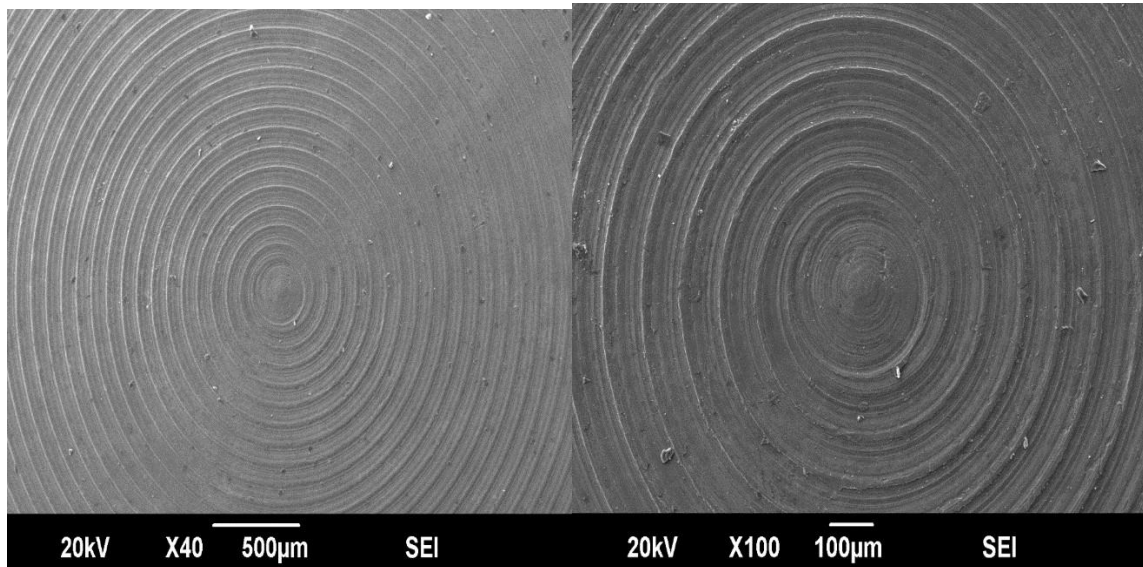
Figure 4 11. SEM images of untreated discs

4.3.2 Seven days Coated Disc

Clusters of nanostar formations are frequently observed in Fig (b), suggesting a uniform covering throughout this disc. For uses like medical implants or catalysis, this kind of surface structure can improve characteristics like surface area and reactivity. In Fig (c) the surface is visible in the SEM image at a 100x magnification. This image offers a wider view of the surface than the previous one at 250x magnification. The overall distribution and regularity of the coating are easier to notice, even with the reduced magnification, while the nanostar structures are still discernible. This even dispersion is essential to maintaining the material's consistent qualities, such increased surface area and possible reactivity. The clusters formed are due to simulated body fluids (SBF) that was coated along with nanostars to enhance the biocompatibility of titanium implants.
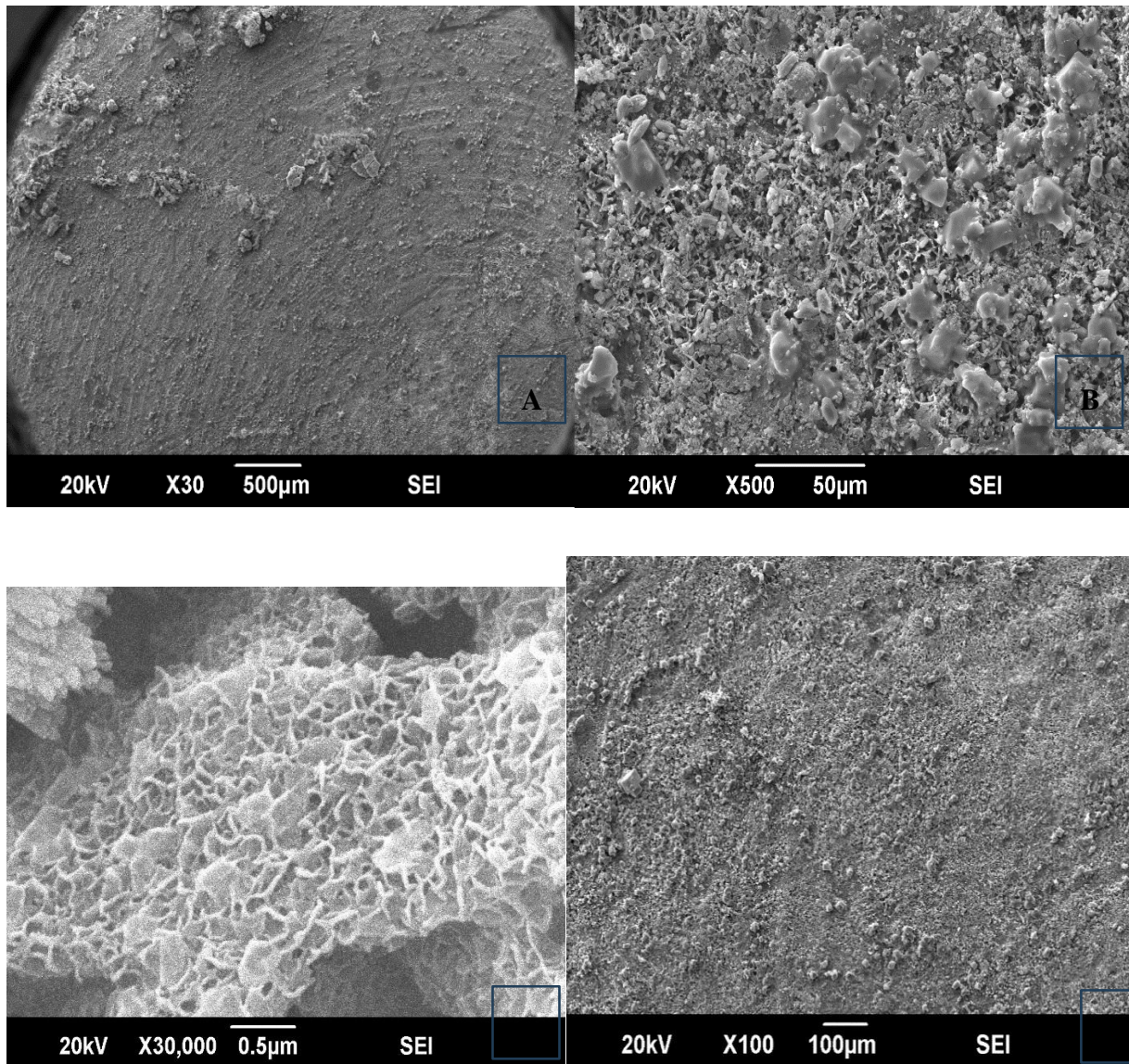
Figure 4 12. (a), (b), (c) and (d): SEM image of multiple layers of silver nanostars and SBF coated for 7 days on titanium discs. The clusters and flakes like structure present in these image are due to SBF.

4.3.3 Fourteen Days Coated disc:

The 14 days coated disc show more even coating of AgNSs on titanium disc. The first image is showing 30 times magnified image of disc while other with 500 and 100 times magnified image. When the material is treated with Simulated Body Fluid (SBF), clusters may form on its surface. Apatite-like crystals grow on the surface of materials, including titanium implants that are

submerged in SBF because the solution replicates the ion concentration of human blood plasma. The calcium phosphate that makes up these clusters typically resembles the mineral hydroxyapatite, which is present in bone. These clusters' development suggests that the surface is bioactive, or that it can form a link with bone tissue that naturally occurs. The characteristics of the material being treated as well as the length of the SBF treatment determine the size, density, and distribution of the clusters.
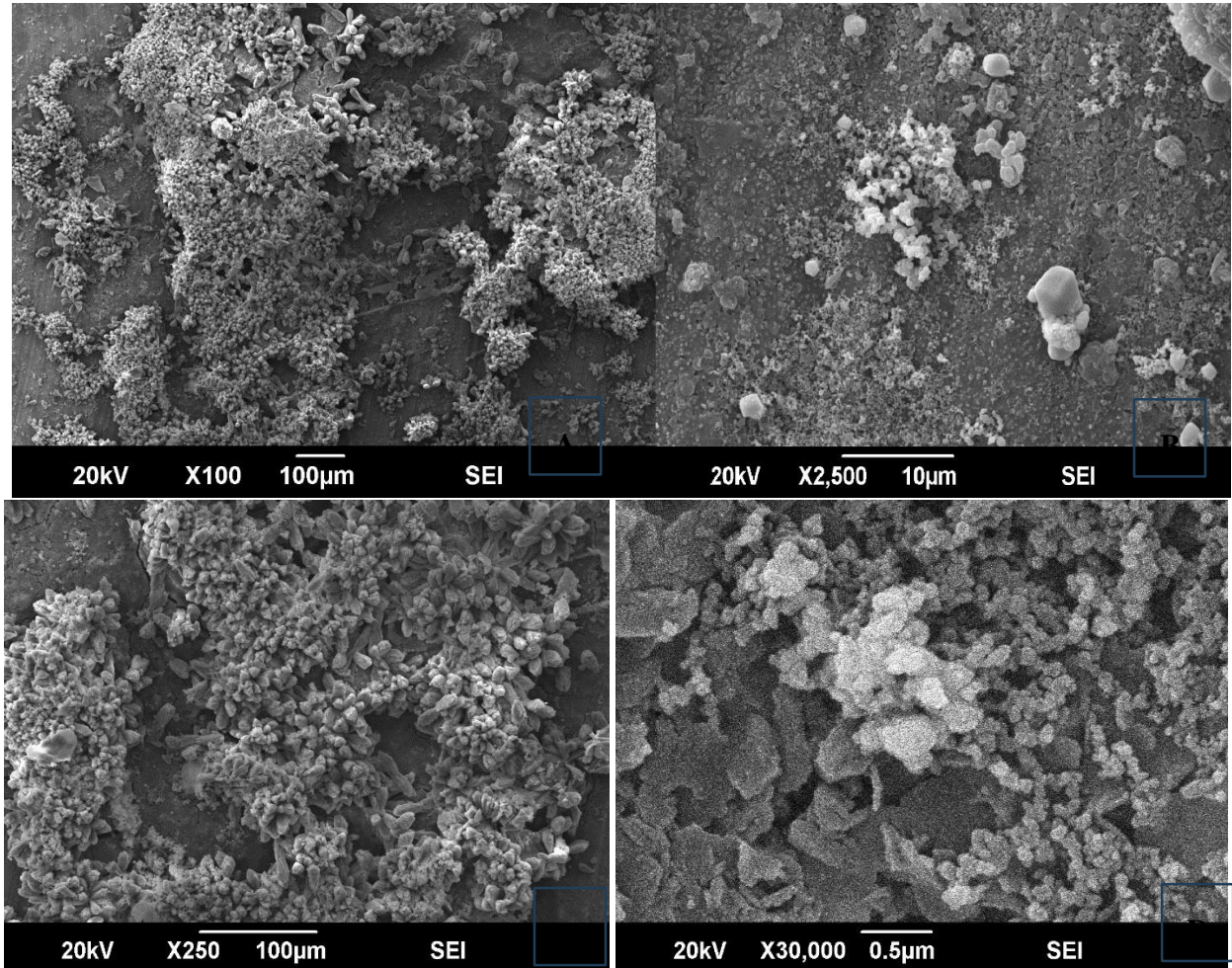
Figure 4.13. A, B, C and D showing images of discs at different magnifications and scale and clearly showing smooth coating of nanoparticles on the discs.

4.4. Contact angle results

Contact angle determines how much hydrophilic or hydrophobic a surface is by estimating the angle between the tangent of liquid drop and solid surface. Contact angle of all three discs was measured and their biocompatibility and oosseointegration was evaluated.

4.4.1. Untreated disc

The contact angle of untreated disc is 68°, which is greater and it is slightly hydrophobic. Water can be drawn to and repelled from the surface to some degree, as indicated by a contact angle of roughly 68°.60. Cell adhesion and protein absorption, which are critical for biocompatibility and Osseo integration, may benefit somewhat from this. Because of its moderate hydrophilicity, the untreated disc offers a respectable but not optimal degree of biocompatibility and Osseo integration potential.
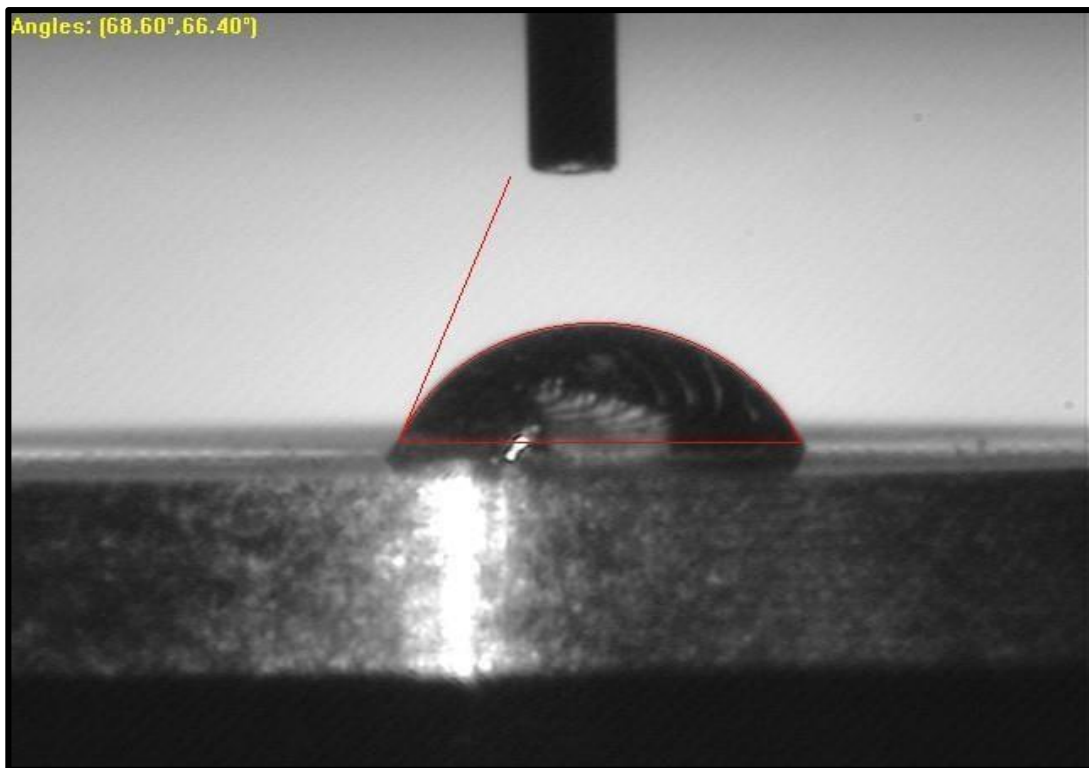
Figure 4.14. Contact angle of 68° indicates moderate hydrophilicity of the disc.

4.4.2. Seven days coated disc

The contact angle of this disc is 38°.10, and with a contact angle of 38°, the surface is very hydrophilic—that is, water is attracted towards it and may readily spread over it. Because it promotes better cell attachment and protein absorption—both of which are necessary for the proper integration of biomedical implants with surrounding tissues—this high degree of hydrophilicity is advantageous for biocompatibility. A low contact angle of 38° in relation to Osseo integration indicates that the surface is appropriate for connecting with bone tissue, enhancing the implant's overall functionality and stability.
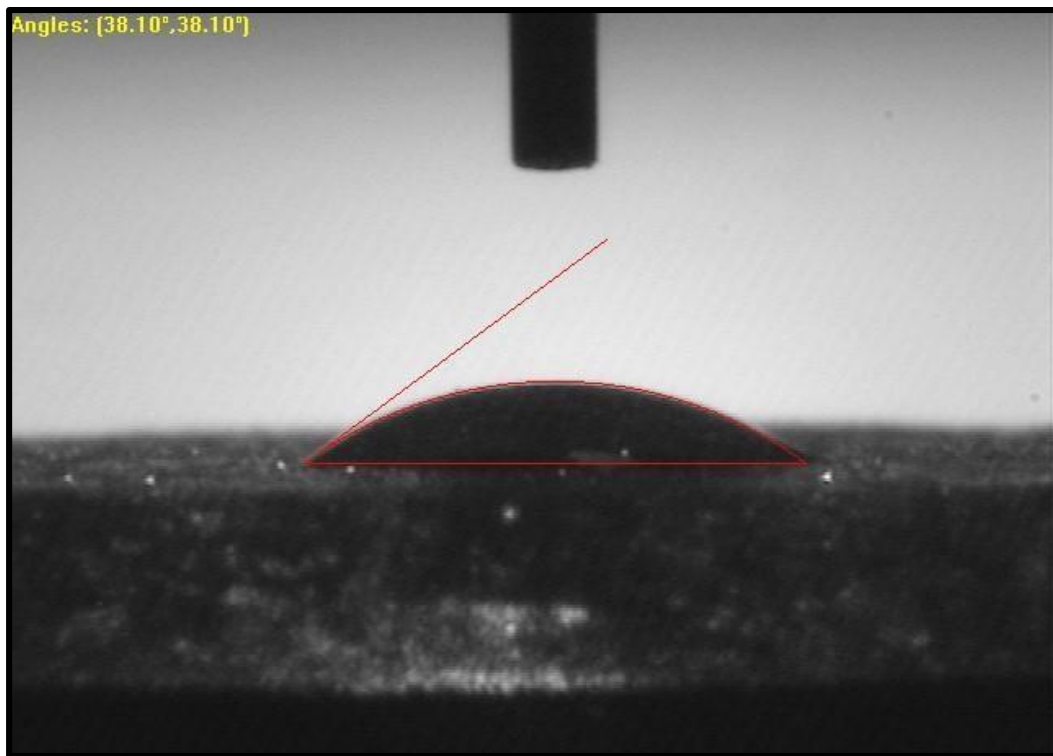
Figure 4.15. Seven days coated disc with contact angle of 38°

4.4.3 Fourteen Days coated disc

A surface having contact angle of 22° is very hydrophilic, meaning it attracts water strongly. Since of the low contact angle, water is more wettable since it travels across the surface more readily. This kind of hydrophilicity enhances protein absorption and cell adhesion, two biocompatibility

factors crucial to the effective integration of medical implants with surrounding tissues. This enhanced wettability also contributes to the form a stable bioactive layer on the surface, enhancing the implant's communication with biological systems. A low contact angle of 22° for Osseo integration improves the material's capacity to adhere to bone tissue, enhancing the implant's long-term durability and performance. All things considered, this high degree of hydrophilicity promotes beneficial biological interactions and enhances the functionality of implants in clinical settings.
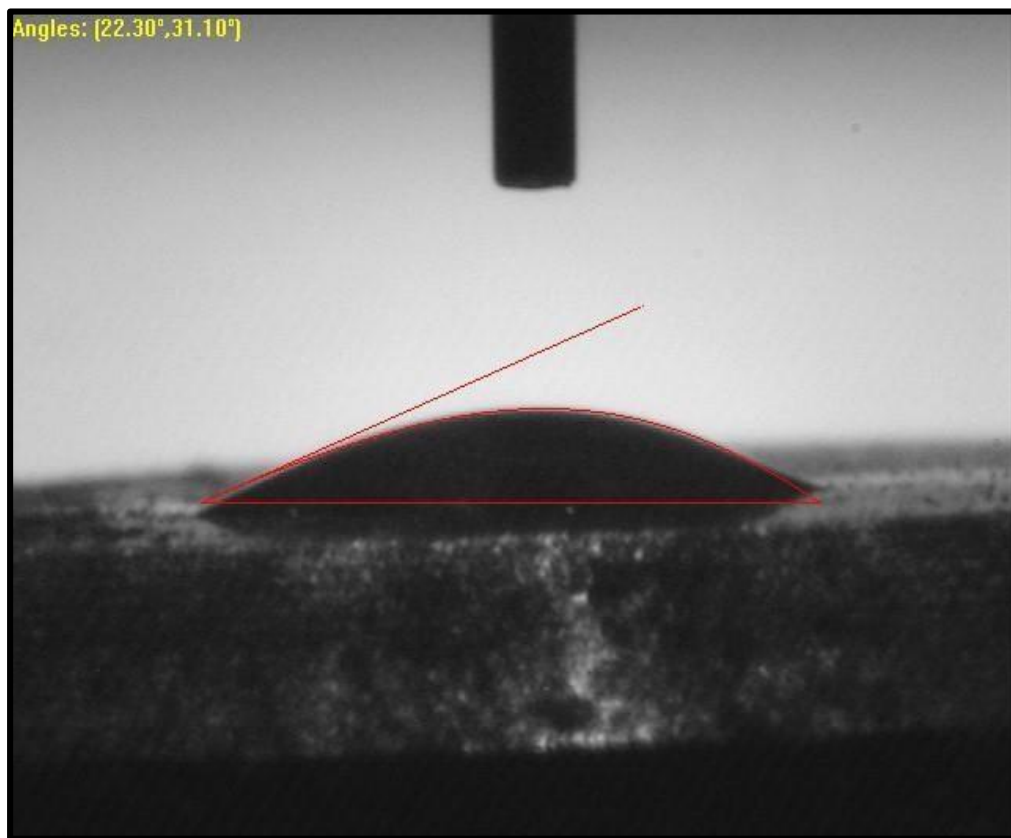
Figure 4.16. Contact angle of fourteen days disc is 22°, which indicates that this is highly hydrophilic and can have excellent biocompatibility.

4.5. Antibiofilm activity of titanium discs against Staphylococcus aureus:

The antibiofilm activity of coated and uncoated titanium disc was evaluated using a microtiter plate spectroscopic experiment in which 96 well plate is used for measuring absorbance of different samples in wells, and they show different absorption depending on the presence of biofilm. The formula for calculating biofilm inhibition is $[(C - B) - (T - B)/(C - B)] * 100$, where C = absorbance of the control (biofilm, no treatment), B = absorbance of blank (only TSB), and T = absorbance of the test (biofilm and treatment), and for my experiment, there were two different treatments so I calculated biofilm inhibition for 7 days and 14 days coated disc separately. 14 Days coated disc shows maximum inhibition (80 to 90%) to biofilm while 7 days disc show moderate biofilm inhibition.

The samples in the well plate show maximum absorption where biofilm was present and from the four samples, maximum absorption was shown by control because it has bacterial culture and minimum absorption was shown by Blank (ethanol) but there was a distinct contrast in absorption of all four samples.

Figure 4.17. Graph showing antibiofilm inhibition of control, 7 days and 14 days discs against *S.aureus* showing good inhibition against biofilm formation.

DISCUSSION

The clinical application of titanium implants, particularly in orthopedics and dentistry, is usually hampered by the bacterial infection risk, which leads to implant failure and severe patient discomfort. The development of antibacterial coatings has become an important point in the field to solve this problem. In this study, we evaluated the potential of using silver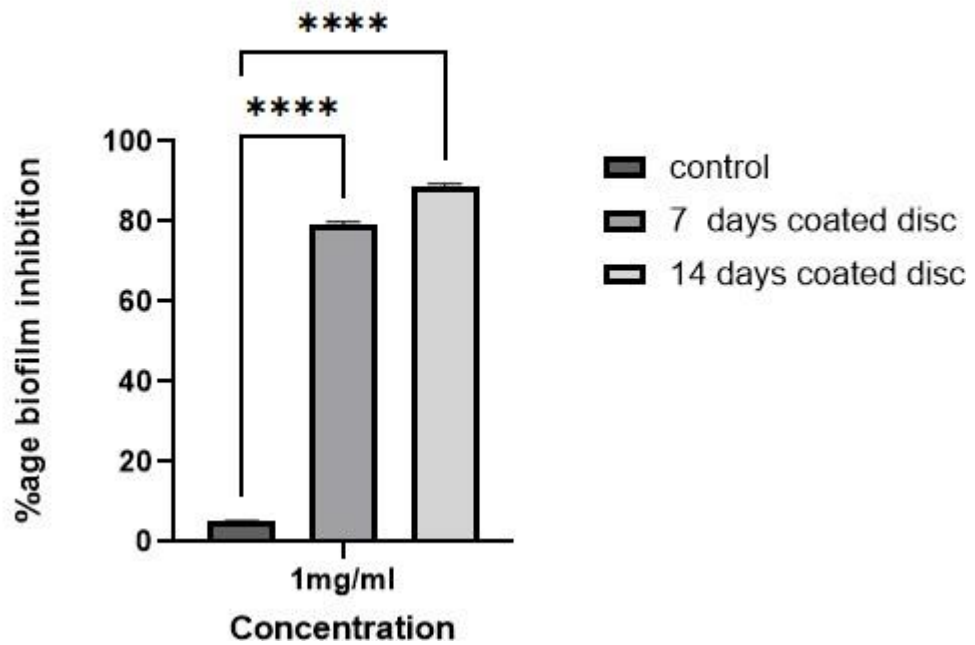 nanostars as a coating material for titanium implants to prevent biofilm formation, a common cause of implant-associated infections. Our results demonstrated a significant reduction in biofilm formation, with 14 days of coated discs being the most effective and reducing biofilm occurrence by approximately 80–90%. The 7-day coated discs also performed well and reduced biofilm formation by 70–80%. These findings conclude that coating duration has a primary role in antibacterial efficacy, with longer coating durations providing a stronger and more stable antibacterial layer. These findings indicate that coating length plays a key role in antibacterial efficacy, with longer coating times resulting in a stronger and more durable antibacterial layer.

The findings support a growing body of research indicating that silver nanoparticles (AgNPs) exhibit antibacterial characteristics when applied on titanium surfaces. Zhang et al. (2020) found that titanium implants coated with silver nanoparticles inhibited biofilms by 85%, specifically against *Staphylococcus aureus*, a frequent pathogen linked with implant infections is a naturally occurring pathogen. This parallelism in inhibition rates suggests that our silver nanostars, with their distinctive star-like form, have equivalent, if not superior, antibacterial activity. The star-like form of our silver nanostars may enhance their antibacterial characteristics. Yang et al. (2018) found that nanostars had a greater impact on bacterial membranes than spherical nanoparticles due to their sharp edges and larger surface area. Abnormal γ forms cause increased interaction with bacterial cells, resulting in membrane penetration and bacterial death. Our findings back up this view, since discs covered with nanostars demonstrated efficient biofilm suppression. Furthermore, the long-term effectiveness reported in discs coated for 14 days is comparable with the findings of Liu et al. (2019), who discovered that long-term exposure to silver on titanium surfaces resulted in prolonged antibacterial activity. This suggests that silver ions are gradually released from nanostars, resulting in a high local concentration of ions that are poisonous to bacteria. The regulated release method guarantees that the antibacterial action is not only instantaneous, but also

long-lasting, which is critical for implant success. Validation of our silver nanostars' characteristics confirmed their effective fabrication and uniform coating on titanium discs. Techniques such as SEM and UV-Vis spectroscopy disclosed well-defined star-like formations with stable size distributions, which is critical for their dependability. X-ray diffraction (XRD) patterns validated the nanostars' crystalline nature, which adds to their durability and usefulness in biological contexts. In comparison to previous research, our nanostars have amazing structural integrity and uniformity. Huang et al. (2020) stressed the importance of nanoparticle stability for long-term use, pointing out that disordered or aggregated particles may lose their antibacterial potency over time. However, our findings indicate that the silver nanostars remained stable and effective even after 14 days of use, which is most likely owing to the better production procedure that we utilized.

 The antibacterial mechanism of silver nanostars has numerous components. Nanostars produce silver ions (Ag^+) that attacks bacterial cell membrane, damage its structure and increase permeability. This contact affects critical cell activities including breathing and reproduction, causing bacterial cell death. Furthermore, silver ions release reactive oxygen species (ROS), which induce free radical stress and kill bacterial cells. Nanostars' vast surface area may increase antibacterial interactions, making them more effective than other silver nanoparticle types. Martínez-Castañón et al. (2008) claimed that silver ions had wide antibacterial action against both Gram-positive and Gram-negative microorganisms. Our 14-day coated discs demonstrated enhanced inhibition, indicating that silver nanoparticles can not only prevent initial bacterial adhesion but also remove existing biofilms that are resistant to traditional therapies.

The clinical implications of the findings are considerable. The ability of silver nanostars to successfully suppress biofilm development on titanium implants suggests a viable technique for reducing implant-associated illnesses. Given the high success rate revealed in our study, silver nanostar coatings may be included into existing implant production processes, adding an extra layer of infection prevention while maintaining biocompatibility. Furthermore, the prolonged antibacterial activity seen with the 14-day coated discs is very important in clinical settings where long-term protection is necessary. This sustained-release technique may lessen the requirement for systemic antibiotics, lowering the danger of antibiotic resistance, which is an increasing problem in clinical practice

CONCLUSIONS

In conclusion, our findings indicate that silver nanostars are an efficient covering material for titanium implants, offering good antibacterial protection against biofilm development. Silver nanoparticles' antibacterial activities include disruption to bacterial cell membranes, the reactive oxygen species production, and huge surface area interactions that are more effective than other types of silver nanoparticles. Furthermore, the narrow contact angle of titanium implants coated with silver nanostars enhances biocompatibility and promotes Osseo integration. The prolonged antibacterial activity of 14-day coated discs demonstrates their potential for long-term therapeutic use, providing considerable advantages in the prevention of implant-associate infections and lowering the requirement for systemic antibiotics. These findings suggest that using silver nanostar coatings in the implant production process can improve the clinical outcomes of titanium implants. Future study should focus on these coatings' in vivo performance and interactions with various bacterial species and host tissues in order to completely show their therapeutic viability.

REFERENCES

1. Statistical Office of the European Communities, *Population Structure and Ageing - Statistics Explained*, 2016. **https://doi.org/http://ec.europa.eu/eurostat/statistics-explained/index.php/Population_structure_and_ageing**

2. Pałka, Krzysztof, and Rafał Pokrowiecki. "Porous titanium implants: a review." *Advanced Engineering Materials* 20, no. 5 (2018): 1700648.

3. Zhang, Lai-Chang, and Liang-Yu Chen. "A review on biomedical titanium alloys: recent progress and prospect." *Advanced engineering materials* 21.4 (2019): 1801215.

4. Leyens, Christoph, and Manfred Peters, eds. *Titanium and titanium alloys: fundamentals and applications*. Wiley-vch, 2006.

5. Niinomi, Mitsuo, and Masaaki Nakai. "Titanium-based biomaterials for preventing stress shielding between implant devices and bone." *International journal of biomaterials* 2011, no. 1 (2011): 836587.

6. W. Nicholson, J. Titanium Alloys for Dental Implants: A Review. *Prosthesis* **2020**, *2*, 100-116. https://doi.org/10.3390/prosthesis2020011

7. Losic, Dusan. "Advancing of titanium medical implants by surface engineering: Recent progress and challenges." *Expert opinion on drug delivery* 18.10 (2021): 1355-1378.

8. Del Castillo, Rafael, Konstantinos Chochlidakis, Pablo Galindo-Moreno, and Carlo Ercoli. "Titanium nitride coated implant abutments: from technical aspects and soft tissue biocompatibility to clinical applications. A literature review." *Journal of Prosthodontics* 31, no. 7 (2022): 571-578.

9. Gepreel, Mohamed Abdel-Hady, and Mitsuo Niinomi. "Biocompatibility of Ti-alloys for long- term implantation." *Journal of the mechanical behavior of biomedical materials* 20 (2013): 407- 415.

10. Mertens, T., and H. Kollek. "On the stability and composition of oxide layers on pre-treated titanium." *International journal of adhesion and adhesives* 30, no. 6 (2010): 466-477.

11. Sidambe, A.T. Biocompatibility of Advanced Manufactured Titanium Implants—A

Review. *Materials* **2014**, *7*, 8168-8188. https://doi.org/10.3390/ma7128168

12. Kopp, Clifford D. "Branemark osseointegration: prognosis and treatment rationale." *Dental Clinics of North America* 33, no. 4 (1989): 701-731.

13. Branemark, Rickard, P. I. Branemark, Björn Rydevik, and Robert R. Myers. "Osseointegration in skeletal reconstruction and rehabilitation: a review." *Journal of rehabilitation research and development* 38, no. 2 (2001): 175-182.

14. Kim, Kyeong Tae, Mi Young Eo, Truc Thi Hoang Nguyen, and Soung Min Kim. "General review of titanium toxicity." *International journal of implant dentistry* 5 (2019): 1-12.

15. Kaur, Manmeet, and K. Singh. "Review on titanium and titanium based alloys as biomaterials for orthopaedic applications." *Materials Science and Engineering: C* 102 (2019): 844-862.

16. Ahmed, Yassin Mustafa, Khairul Salleh Mohamed Sahari, Mahadzir Ishak, and Basim Ali Khidhir. "Titanium and its alloy." *International Journal of Science and Research* 3, no. 10 (2014): 1351-1361.

17. Veiga, Celestino, J. Paulo Davim, and A. J. R. Loureiro. "Properties and applications of titanium alloys: a brief review." *Rev. Adv. Mater. Sci* 32, no. 2 (2012): 133-148.

18. Rack, H. J., and J. I. Qazi. "Titanium alloys for biomedical applications." *Materials Science and Engineering: C* 26, no. 8 (2006): 1269-1277.

19. Fan, Zhechao, and Hongwei Feng. "Study on selective laser melting and heat treatment of Ti-6Al-4V alloy." *Results in Physics* 10 (2018): 660-664.

20. Dziubińska, Anna & Majerski, Krzysztof & Winiarski, Grzegorz. (2017). Investigation of the Effect of Forging Temperature on the Microstructure of Grade 5 Titanium ELI. Advances in Science and Technology Research Journal. 11. 147-158. 10.12913/22998624/76488.

21. Hong, Shane Y., Irel Markus, and Woo-cheol Jeong. "New cooling approach and tool life improvement in cryogenic machining of titanium alloy Ti-6Al-4V." *International journal of machine tools and manufacture* 41, no. 15 (2001): 2245-2260.

22. Leyens, Christoph, and Manfred Peters, eds. *Titanium and titanium alloys: fundamentals and applications*. Wiley-vch, 2006.

23. 4. Liliane S. Morais et al., "Titanium Alloy Mini-Implants for Orthodontic Anchorage: Immediate Loading and Metal Ion Release," Acta Biomaterialia, 3 (3) (2007), pp. 331–339.

23.] Effah, E. A. B., P. D. Bianco, and P. Ducheyne. "Crystal structure of the surface oxide layer on titanium and its changes arising from immersion." *Journal of biomedical materials research* 29, no. 1 (1995): 73-80.

25. Al-Hashedi, Ashwaq A., Marco Laurenti, Veronique Benhamou, and Faleh Tamimi. "Decontamination of titanium implants using physical methods." *Clinical oral implants research* 28, no. 8 (2017): 1013-1021.

26. Balshe, Ayman A., Daniel A. Assad, Steven E. Eckert, Sreenivas Koka, and Amy L. Weaver. "A Retrospective Study of the Survival of Smoothand Rough-Surface Dental Implants." *International Journal of Oral & Maxillofacial Implants* 24, no. 6 (2009).

27. Moran, E., I. Byren, and B. L. Atkins. "The diagnosis and management of prosthetic joint infections." *Journal of antimicrobial chemotherapy* 65, no. suppl_3 (2010): iii45-iii54.

28. Norowski Jr, P. Andrew, and Joel D. Bumgardner. "Biomaterial and antibiotic strategies for peri-implantitis: A review." *Journal of Biomedical Materials Research Part B: Applied Biomaterials: An Official Journal of The Society for Biomaterials, The Japanese Society for Biomaterials, and The Australian Society for Biomaterials and the Korean Society for Biomaterials* 88, no. 2 (2009): 530-543.

29. Hori, Katsutoshi, and Shinya Matsumoto. "Bacterial adhesion: From mechanism to control." *Biochemical Engineering Journal* 48, no. 3 (2010): 424-434.

30. Lindsay, D., and A. Von Holy. "Bacterial biofilms within the clinical setting: what healthcare professionals should know." *Journal of Hospital Infection* 64, no. 4 (2006): 313-325.

31. Dorkhan, Marjan, Luis E. Chávez de Paz, Marie Skepö, Gunnel Svensäter, and Julia R. Davies. "Effects of saliva or serum coating on adherence of Streptococcus oralis strains to titanium." *Microbiology* 158, no. 2 (2012): 390-397.

32. Hämmerle, C. H. "Biofilm on dental implants: a review of the literature." *Int. J. Oral Maxillofac Implant* 24 (2009): 616.

33. Pallavicini, Piersandro, Giacomo Dacarro, and Angelo Taglietti. "Self-assembled monolayers of silver nanoparticles: from intrinsic to switchable inorganic antibacterial surfaces." *European Journal of Inorganic Chemistry* 2018, no. 45 (2018): 4846-4855.

34. Wahab, S.; Khan, T.; Adil, M.; Khan, A. Mechanistic Aspects of Plant-Based Silver Nanoparticles against Multi-Drug Resistant Bacteria. *Heliyon* **2021**, *7*, e07448. [**Google Scholar**] [**CrossRef**] [**PubMed**]

35. Dakal, Tikam Chand, Anu Kumar, Rita S. Majumdar, and Vinod Yadav. "Mechanistic basis of antimicrobial actions of silver nanoparticles." *Frontiers in microbiology* 7 (2016): 1831.

36. S.L., Wang., Fanping, Meng., Zhimin, Cao. (2024). Improving Surface Antimicrobial Performance by Coating Homogeneous PDA-Ag Micro–Nano Particles. Coatings, 14(7), 887-887. doi: 10.3390/coatings14070887

37. Aya, Ali., Likhitha, Polepalli., Sheetal, Chowdhury., Mary, A., Carr., Amol, V., Janorkar.,

Mary, E., Marquart., Jason, A., Griggs., Joel, D., Bumgardner., Michael, D., Roach. (2024). Silver-Doped Titanium Oxide Layers for Improved Photocatalytic Activity and Antibacterial Properties of Titanium Implants. Journal of Functional Biomaterials, 15(6), 163-163. doi: 10.3390/jfb15060163

38. Everton, Granemann, Souza., Chiara, das, Dores, do, Nascimento., César, Aguzzoli., Elena, Sarai, Baena, Santillán., Carlos, Enrique, Cuevas-Suárez., Patrícia, da, Silva, Nascente., Evandro, Piva., Rafael, Guerra, Lund. (2024). Enhanced Antibacterial Properties of Titanium Surfaces through Diversified Ion Plating with Silver Atom Deposition. Journal of Functional Biomaterials, 15(6), 164-164. doi: 10.3390/jfb15060164

38. Chen, Jiao, Huang., Haiyan, Wang., Lili, Yao., Li, Li., Wei, Wei, Lou., Litao, Yao., Yitian, Shi., Renren, Li. (2024). (4) Fabrication and evaluation of silver modified micro/nano structured titanium implant.. Journal of Biomaterials Applications, doi: 10.1177/08853282231222590

39. Daniel, Ospina, Moreno., Judit, Buxadera-Palomero., Maria-Pau, Ginebra., José, María, Manero., Helena, Martin-Gómez., Carlos, Mas-Moruno., Daniel, Rodríguez. (2023). Comparison of the Antibacterial Effect of Silver Nanoparticles and a Multifunctional Antimicrobial Peptide on Titanium Surface. International Journal of Molecular Sciences, 24(11), 9739-9739. doi: 10.3390/ijms24119739

40. Irem, Cemre, Turu., Semih, Bayraktar., Busra, Akgul., Esra, Ilhan-Sungur., Emrah, Sefik, Abamor., Nurhan, Cansever. (2023). Formation of TiO2 nanotubes and deposition of silver nanoparticle and reduced graphene oxide: Antibacterial and biocompatibility behavior. Surface & Coatings Technology, doi: 10.1016/j.surfcoat.2023.129866

41. Jian, Xiong., Long, Zhang., Lei, Yu., Qiying, Lv. (2023). Using laser etched-array periodic structure surface to construct silver loaded titanium implants with combined efficient

antibacterial and osteogenic properties. Applications of Surface Science, doi: 10.1016/j.apsusc.2023.158533

42. Bakhtikhon, Kurbonova. (2023). Evaluation of the performance of TiO2 thin films doped with silver nanoparticles as a protective coating for metal prostheses. Surface & Coatings Technology,

458, 129349-129349. doi: 10.1016/j.surfcoat.2023.129349

43. Sepúlveda, Borja, Paula C. Angelomé, Laura M. Lechuga, and Luis M. Liz-Marzán. "LSPR-based nanobiosensors." *Nano today* 4, no. 3 (2009): 244-251.

44. Barani, Hossein, and Boris Mahltig. "Microwave-assisted synthesis of silver nanoparticles: Effect of reaction temperature and precursor concentration on fluorescent property." *Journal of Cluster Science* (2022): 1-11.

45. Revnic, Radu Nicolae, Gabriela Fabiola Ştiufiuc, Valentin Toma, Anca Onaciu, Alin Moldovan, Adrian Bogdan Ţigu, Eva Fischer-Fodor, Romulus Tetean, Emil Burzo, and Rareş Ionuţ Ştiufiuc. 2022. "Facile Microwave Assisted Synthesis of Silver Nanostars for Ultrasensitive Detection of Biological Analytes by SERS" *International Journal of Molecular Sciences* 23, no. 15: 8830. https://doi.org/10.3390/ijms23158830

46. Thu, Vu Thi, Nguyen Manh Cuong, Dao Tran Cao, Luu Tien Hung, and Luong Truc-Quynh Ngan. "Trace detection of ciprofloxacin antibiotic using surface-enhanced Raman scattering coupled with silver nanostars." *Optik* 260 (2022): 169043.

47. Reyes Gómez, Faustino, Rafael J. G. Rubira, Sabrina A. Camacho, Cibely S. Martin, Robson R. Da Silva, Carlos J. L. Constantino, Priscila Alessio, Osvaldo N. Oliveira, Jr., and J. Ricardo Mejía-Salazar. 2018. "Surface Plasmon Resonances in Silver Nanostars" *Sensors* 18, no. 11: 3821. https://doi.org/10.3390/s18113821

48.   Tang, Shaoheng , and Jie Zheng. "Antibacterial activity of silver nanoparticles: structural effects." *Advanced healthcare materials* 7, no. 13 (2018): 1701503.

49.   Dakal, Tikam Chand, Anu Kumar, Rita S. Majumdar, and Vinod Yadav. "Mechanistic basis of antimicrobial actions of silver nanoparticles." *Frontiers in microbiology* 7 (2016): 1831.

50.   Khodashenas, Bahareh, and Hamid Reza Ghorbani. "Synthesis of silver nanoparticles with different shapes." *Arabian Journal of Chemistry* 12, no. 8 (2019): 1823-1838.